Accepted Manuscript

Synthesis and biological evaluation of *N*-substituted 3-oxo-1,2,3,4- tetrahydro-quinoxaline-6-carboxylic acid derivatives as tubulin polymerization inhibitors

Jianguo Qi, Haiyang Dong, Jing Huang, Shufeng Zhang, Linqiang Niu, Yahong Zhang, Jianhong Wang

PII: S0223-5234(17)30621-9

DOI: 10.1016/j.ejmech.2017.08.018

Reference: EJMECH 9662

To appear in: *European Journal of Medicinal Chemistry*

Received Date: 2 October 2016

Revised Date: 5 August 2017

Accepted Date: 6 August 2017

Please cite this article as: J. Qi, H. Dong, J. Huang, S. Zhang, L. Niu, Y. Zhang, J. Wang, Synthesis and biological evaluation of *N*-substituted 3-oxo-1,2,3,4- tetrahydro-quinoxaline-6-carboxylic acid derivatives as tubulin polymerization inhibitors, *European Journal of Medicinal Chemistry* (2017), doi: 10.1016/ j.ejmech.2017.08.018.

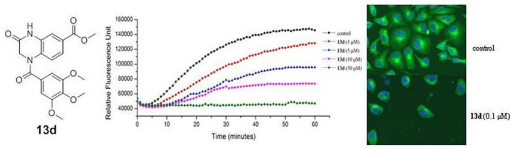

Synthesis and Biological Evaluation of *N*-substituted 3-oxo-1,2,3,4-tetrahydro-quinoxaline-6-carboxylic Acid Derivatives as Tubulin Polymerization Inhibitors

Jianguo Qi [a], Haiyang Dong [a], Jing Huang [a], Shufeng Zhang [a], Linqiang Niu [a], Yahong Zhang [a, *], Jianhong Wang [a, *]

[a] Key Laboratory of Natural Medicine and Immuno-Engineering of Henan Province, Henan University Jinming Campus, Kaifeng 475004, Henan, China

* Corresponding author

E-mail address: zhangyahong_131@163.com, jhworg@126.com

Abstract

A series of novel *N*-substituted 3-oxo-1,2,3,4-tetrahydro-quinoxaline-6-carboxylic acid derivatives were synthesized and evaluated for their biological activities. Among all synthesized target compounds, **13d** exhibited the most potent antiproliferative activity against HeLa, SMMC-7721, K562 cell line (IC_{50} = 0.126 μM, 0.071 μM, 0.164 μM, respectively). Furthermore, compound **13d** inhibited tubulin polymerization (IC_{50} = 3.97 μM), arrested cell cycle at the G2/M phase and induced apoptosis. The binding mode at the colchicine binding site was also probed. These studies provided a new molecular scaffold for the further development of antitumor agents that target tubulin.

Keywords

Antiproliferative; Tubulin polymerization inhibitors; Cell cycle analysis; Cell apoptosis; 3-Oxo-1,2,3,4-tetrahydro-quinoxaline-6-carboxylic acid derivatives.

1. Introduction

Microtubules, which are dynamic polymers of αβ-tubulin, play an essential role in mitosis, forming the dynamic spindle apparatus. Disruption of microtubule dynamics prevents microtubule function and ultimately leads to cell death. This made microtubules an important target for cancer chemotherapy. Microtubule-targeting agents are divided into two groups, microtubule-stabilizing agents (paclitaxel, laulimalide etc) and tubulin polymerization inhibitors (vinca alkaloids, colchicine etc). These agents interact with tubulin through three major binding sites, vinca alkaloid-, taxane- and colchicine-binding sites [1-3]. Recently, diverse small molecules that act at the colchicine site on tubulin have come under intensive investigation. These compounds not only display potent cytotoxicity against a wide variety of human cancer cell lines but also show selective toxicity toward tumor endothelial cells required for the growth of the cancer. Thus they represent a new class of vascular disrupting agents which cause a significant shutdown of the blood vessels of tumors, leading to cancer cell death via necrosis and apoptosis. Moreover, they show promising ability to overcome multidrug resistance mediated by P-glycoprotein [4-14]. Therefore, this type of tubulin inhibitor might provide a new opportunity for cancer therapy.

Currently, some drug candidates targeting at the colchicine site are in clinical development. CA4-P (**1a**, Figure 1), the phosphate derivative prodrug of combretastatin A-4 (CA-4, **1b**, Figure 1), has entered clinical trials either alone or in combination with other chemotherapeutic agents [15, 16]. However, the cis-stilbene of CA-4 is prone to isomerisation into its inactive trans-form during storage and administration. To avoid the stability problems of CA-4, many conformationally restricted modification have been used [17-23]. Phenstatin (**2**, Figure 1) which is the CA-4 analogue with the double bond of CA-4 being replaced by a carbonyl group showed strong cytotoxicity and antitubulin activity similar to CA-4, but it is more stable compared with CA-4 [24]. BNC-105P (**3a**, Figure 1), developed by Bionomics (Australia), is a phosphorylated prodrug of BNC-105 (**3b**, Figure 1) and it entered clinical trials in combination with everolimus for progressive metastatic clear cell

renal cell carcinoma. It is the phenstatin analogue with the benzene ring (ring B) of phenstatin being replaced by coumarone [25]. Based on BNC-105 and other modification of CA-4 and phenstatin, we conclude that ring B could be replaced by other heterocycles, such as chromane, indole etc [26-41].

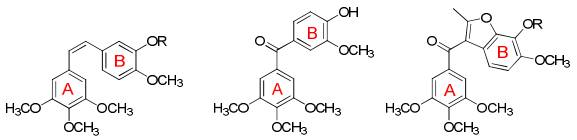

1a (CA-4P) R = $P(O)O_2Na_2$
1b (CA-4) R = H
2 (Phenstatin)
3a (BCN-105) R = $P(O)O_2Na_2$
3b (BCN-105P) R = H

Figure 1. CA-4 and its analogues targeting at the colchicine site of tubulin.

Quinoxalinone structure has good physico-chemical properties and drug-like properties. Many bioactive compounds contain this moiety [42, 43]. The current study was undertaken to investigate the in vitro antitumor activity of a novel modification of phenstatin. The replacement of one phenyl ring with 3-oxo-1,2,3,4-tetrahydro-quinoxaline-6-carboxylic acid and its derivatives were pursued. Herein we report the synthesis and biological evaluation of a series of *N*-substituted 3-oxo-1,2,3,4-tetrahydro-quinoxaline-6-carboxylic acid derivatives. Compound **13d** was identified with IC_{50} values ranging from 0.071 to 0.164 μM against the three cancer cell lines. The effects on tubulin polymerization, cell cycle and apoptosis were also evaluated.

2. Results and discussion

2.1. Chemistry

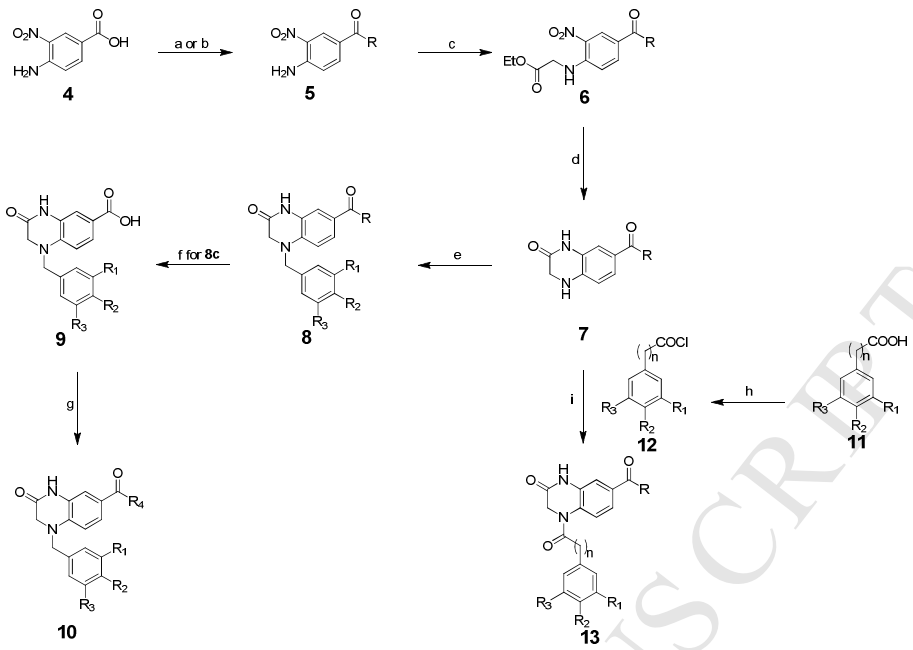

5a/6a/7a: R = -OCH3
5b/6b/7b: R = 
5c/6c/7c: R = 
5d/6d/7d: R = 
5e/6e/7e: R = 

11a/12a: $R_1 = R_3 =$ -H $R_2 =$ -F n = 0
11b/12b: $R_1 = R_3 =$ -H $R_2 =$ -OCH3 n = 0
11c/12c: $R_1 = R_2 =$ -OCH3 $R_3 =$ -H n = 0
11d/12d: $R_1 = R_2 = R_3 =$ -OCH3 n = 0
11e/12e: $R_1 = R_2 = R_3 =$ -OCH3 n = 1

8a: $R = R_2 =$ -OCH3 $R_1 = R_3 =$ -H
8b: $R = R_1 = R_2 =$ -OCH3 $R_3 =$ -H
8c: $R = R_1 = R_2 = R_3 =$ -OCH3

9: $R_1 = R_2 = R_3 =$ -OCH3

10a: $R_1 = R_2 = R_3 =$ -OCH3 $R_4 =$ 
10b: $R_1 = R_2 = R_3 =$ -OCH3 $R_4 =$ 

13a: R = -OCH3 $R_1 = R_3 =$ -H $R_2 =$ -F n = 0
13b: R = -OCH3 $R_1 = R_3 =$ -H $R_2 =$ -OCH3 n = 0
13c: R = -OCH3 $R_1 = R_2 =$ -OCH3 $R_3 =$ -H n = 0
13d: R = -OCH3 $R_1 = R_2 = R_3 =$ -OCH3 n = 0
13e: R = -OCH3 $R_1 = R_2 = R_3 =$ -OCH3 n = 1
13f: R =  $R_1 = R_2 =$ -OCH3 $R_3 =$ -H n = 0
13g: R =  $R_1 = R_2 = R_3 =$ -OCH3 n = 0
13h: R =  $R_1 = R_2 = R_3 =$ -OCH3 n = 0
13i: R =  $R_1 = R_2 =$ -OCH3 $R_3 =$ -H n = 0
13j: R =  $R_1 = R_2 = R_3 =$ -OCH3 n = 0
13k: R =  $R_1 = R_2 =$ -OCH3 $R_3 =$ -H n = 0
13l: R =  $R_1 = R_2 = R_3 =$ -OCH3 n = 0

Scheme 1. Reagents and conditions: a) $SOCl_2$, MeOH, 0-50 ^oC; b) amines, EDCI, CH_2Cl_2, rt; c) ethyl bromoacetate, Cs_2CO_3, 140 ^oC; d) 10% Pd/C, H_2, MeOH, rt; e) benzyl chlorides, KI, K_2CO_3, CH_3CN, 70 ^oC; f) LiOH, THF, H_2O, 40 ^oC; g) oxalyl chloride, PhMe, 70 ^oC; amines, K_2CO_3, THF, rt; h) $SOCl_2$, 70 ^oC; i) **12a-e**, K_2CO_3, THF, rt.

Scheme 1 depicts the synthetic pathways used for the preparation of quinoxalinone derivatives. Starting from the commercial compound 4-amino-3-nitrobenzoic acid (**4**), the reaction with thionyl chloride in methanol and properly substituted amines in the presence of 1-ethyl-3-(3-dimethylaminopropyl)carbodiimide

hydrochloride (EDCI) in CH_2Cl_2 provided the compounds **5a-5e** (71.8% – 89.2%). These latter compounds reacted with ethyl bromoacetate in the presence of Cs_2CO_3 to afford compounds **6a-6e** (44.3% – 58.3%). The key intermediates **7a-7e** (68.8% – 82.4%) were synthesized via a "one pot" reduction of the nitro group using hydrogen in the presence of palladium on charcoal and cyclization reaction of **6a-6e** in methanol. Compounds **8a-8c** (42.3% – 67.8%) were prepared by nucleophilic substitution of substituted benzyl chlorides with intermediates **7a-7e** using K_2CO_3 as a base. The subsequent hydrolysis of compound **8c** using LiOH aqueous solution furnished the desired compound **9** (72.6%). Compound **9** was converted into its acid chloride with oxalyl chloride in toluene. Compounds **10a** (73.2%) and **10b** (62.4%) were prepared by condensation of the acid chloride mentioned above with properly substituted amines in the presence of K_2CO_3 in tetrahydrofuran (THF). Compounds **13a-13i** (46.7% – 65.3%) were prepared by nucleophilic addition of intermediates **7a-7e** with substitued benzoyl chlorides in the presence of K_2CO_3 in THF. The benzoyl chlorides **12a-12e** were gained by treatment of substituted benzoic acids with thionyl chloride.

2.2. Biological evaluation

2.2.1. In vitro antiproliferative activity

The in vitro antiproliferative activities of the synthesized target compounds were evaluated against HeLa (human epithelial cervical cancer), SMMC-7721(human hepatoma cancer), and K562 (leukemia) cell lines using MTT assay. Doxorubicin and CA-4 were chosen as reference drugs. The results are summarized in Table 1. The antiproliferative activities of the compounds were expressed as the concentration of compounds required for 50% inhibition of cell growth (IC_{50}). IC_{50} values were calculated from at least five different concentrations of test compounds.

Table 1. The in vitro antiproliferative activities of synthesized target compounds (**8a-8c**, **9**, **10a**, **10b**, **13a-13l**, doxorubicin and CA-4 against three human cancer cell lines (HeLa, SMMC-7721 and K562)

Compound	Antiproliferative Activity (IC_{50}, μM)		
	HeLa	SMMC-7721	K562
8a	16.4±1.5	12.5±1.3	43.2±2.9
8b	38.1±5.0	33.2±2.5	43.6±0.7
8c	2.76±0.50	2.69±0.45	3.42±0.85
9	32.2±4.7	39.0±3.9	35.9±8.5
10a	37.5±3.1	39.7±2.3	43.0±7.2
10b	41.8±1.9	28.0±5.4	42.6±4.5
13a	15.9±1.8	7.69±0.35	9.80±2.17
13b	8.28±1.43	5.40±0.78	7.72±2.70
13c	1.42±0.25	1.32±0.22	3.00±1.05
13d	0.126±0.015	0.071±0.014	0.164±0.005
13e	39.4±5.1	9.10±1.68	45.3±3.5
13f	> 50	> 50	> 50
13g	> 50	43.1±7.6	> 50
13h	> 50	40.6±1.7	> 50
13i	24.9±2.4	34.4±3.1	42.9±4.0
13j	26.4±7.4	37.9±8.3	> 50
13k	34.9±7.5	34.9±7.9	> 50
13l	> 50	39.2±7.6	> 50
doxorubicin	1.82±0.31	1.59±0.27	0.89±0.17
CA-4	0.013±0.003	0.0038±0.0020	0.013±0.001

As shown in Table 1, most of the synthesized compounds inhibited the growth of the three cancer cells with IC_{50} values under 50 μM. The comparison of IC_{50} values of

8a – **8c** demonstrated that **8c** which had 3,4,5-trimethoxybenzyl substitution on the nitrogen atom of methyl 3-oxo-1,2,3,4-tetrahydroquinoxaline-6-carboxylate had better activity than **8a** (4-methoxybenzyl) and **8b** (3,4-dimethoxybenzyl). The activity decreased by an order of magnitude when the methyl carboxylate of **8c** was hydrolyzed to carboxylic acid (**9**). Compound **10a** or **10b** with *N*-butyl or *N*-cyclohexyl quinoxalinone-6-carboxamide substitued for quinoxalinone-6-carboxylate of compound **8c** showed comparable activity with compound **9**.

Comparison of compounds **13b** – **13d** with compounds **8a** – **8c** revealed that the replacement of benzyl group with benzoyl group led to a remarkable improvement in antiproliferative activity of the corresponding compounds. The antiproliferative activity of compounds **13b** – **13d** with different substituents on the benzene increased in the following order: **13d** (3,4,5-trimethoxy) > **13c** (3,4-dimethoxy) > **13b** (4-methoxy). Compounds **13d** and **13c** were the two most potent compounds among all the synthesized target compounds. Compound **13d** exhibited better activity than doxorubicin, but less than CA-4. Compound **13a** with para-fluoro substituent on the phenyl ring showed comparable activity with **13b** (4-methoxy). Lengthening the benzoyl moiety of **13d** to phenylacetyl group (**13e**) caused a significant reduction in antiproliferative activity in all cell lines. Replacement of methyl carboxylate on the quinoxalinone with amide (**13f-13l**) led to weak activity.

2.2.2. In vitro inhibition of tubulin polymerization

Three compounds, including **8c**, **13c** and **13d**, were selected to evaluate for their ability to inhibit tubulin polymerization and they were employed at 20 μM in the assay. CA-4 (2.5 μM) and paclitaxel (3 μM) were evaluated as reference compounds. Compound **13d** was employed at four different concentrations in order to determine the IC_{50}. In the assay, the IC_{50} was defined as the concentration of compound that inhibited 50% the extent of assembly of 10 μM tubulin after 40 min incubation at 37 ^{o}C. As shown in figure 2A, **8c**, **13c** and **13d** resulted in various degrees of inhibition of tubulin polymerization compared with control (0.1% DMSO). Compound **13d** inhibited tubulin polymerization with an IC_{50} value of 3.97 μM.

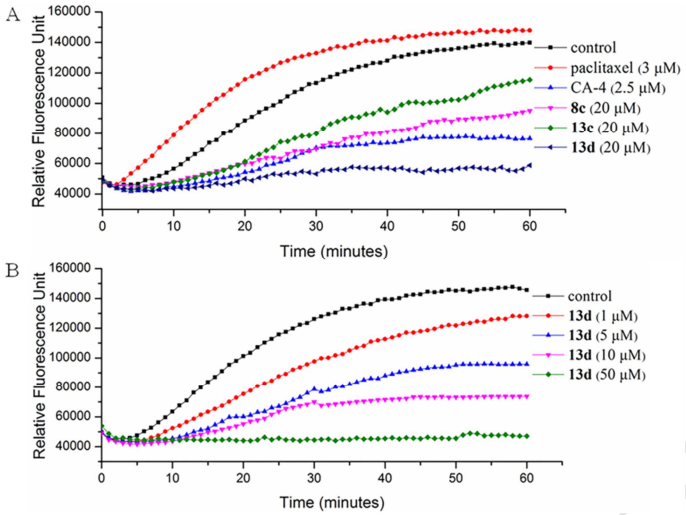

Figure 2. (A) Effects of 20 μM **8c**, **13c** and **13d** on tubulin polymerization. Paclitaxel (3 μM) and CA-4 (2.5 μM) were used as reference drugs, 0.1% DMSO as control. (B) Inhibition of tubulin polymerization by **13d** with different concentrations (1 μM, 5 μM, 10 μM, 50 μM).

2.2.3. Antimicrotubule effects in heLa cells

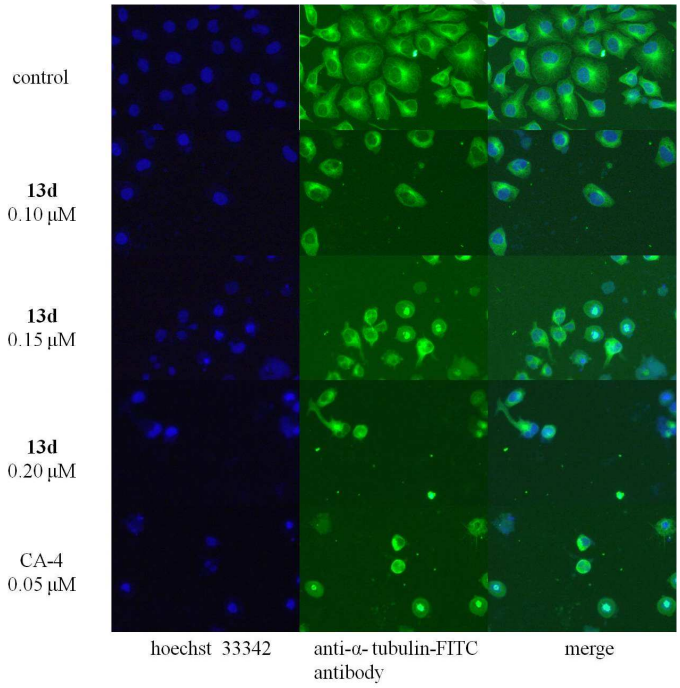

Figure 3. Fluorescence microscopic images of HeLa cells stained with Hoechst 33342 or anti-α-tubulin-FITC antibody after treatment with 0.1% DMSO, **13d** (0.10 μM, 0.15 μM, 0.20 μM) or CA-4 (0.05 μM) for 24 h.

Compound **13d** was selected to evaluate the effects on microtubule assembly in the cell-based phenotypic assay. HeLa cells were treated with three different concentrations (0.10 μM, 0.15 μM, 0.20 μM) of **13d** or 0.05 μM CA-4 for 24 h. Cells

were stained with Hoechst 33342 and anti-α-tubulin-FITC antibody. As shown in figure 3, the cells without drug treatment exhibited normal filamentous microtubules arrays, with microtubules extending to the peripheral region of the cells. The cells treated with drugs exhibited reduced microtubule networks. Compound **13d** induced a dose-dependent collapse of the microtubule network.

2.2.4. Effect on cell cycle progression

Inhibition of tubulin polymerization leads to G2/M cell cycle arrest. Compound **13d** was evaluated in dose-response experiments for study on cell cycle distribution. HeLa cells were treated with four different concentrations (0.10 μM, 0.15 μM, 0.20 μM, 0.25 μM) of **13d** for 24 h. As shown in Figure 4, compound **13d** induced a significant increase in the proportion of cells in the G2/M phase based on DNA content at 0.15μM. Most cells accumulated in G2/M phase at 0.25 μM. It was concluded that compound **13d** caused G2/M cell cycle arrest in a concentration-dependent manner.

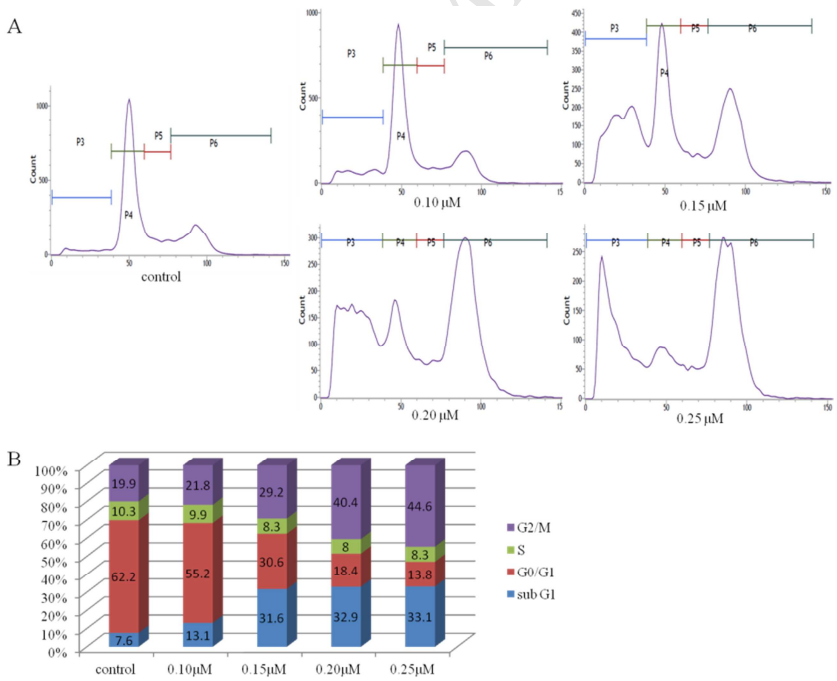

Figure 4. (A) Flow cytometry analysis of HeLa cells treated with 0.1% DMSO, 0.10 μM, 0.15 μM, 0.20 μM or 0.25 μM compound **13d** for 24 h. (B) The statistical graph of cell cycle distribution.

2.2.5. Compound 13d induce apoptosis

To investigate the mode of cell death induced by **13d**, the annexin V/propidium

iodide (PI) double staining assay was performed. HeLa cells were treated with three different concentrations of **13d** for 24 h. As depicted in figure 5, the four quadrants represented live cells (annexin-V^-/PI^-), early apoptotic cells (annexin-V^+/PI^-), late apoptotic cells (annexin-V^+/PI^+), and necrotic cells (annexin-V^-/PI^+). It was concluded that **13d** induced an accumulation of annexin-V positive cells in comparison with the control group, in a concentration dependent manner. Cell shrinkage, membrane blebbing and plasmatorrhexis that imply the cell apoptosis could be observed under the microscope.

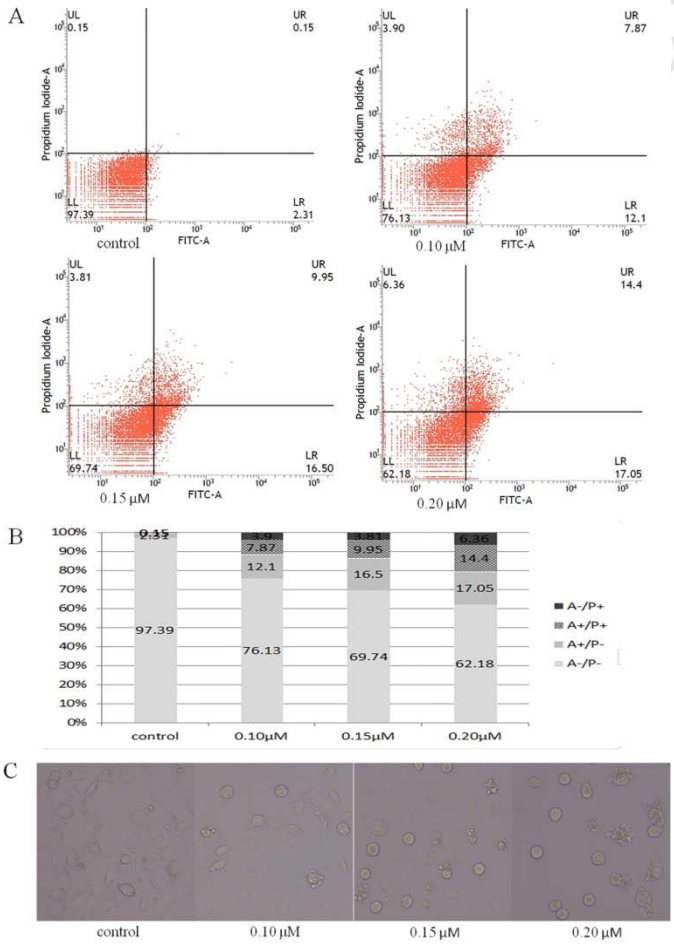

Figure 5. (A) Bi-parametric histograms of HeLa cells treated with 0.1% DMSO, 0.10 μM, 0.15 μM or 0.20 μM compound **13d** for 24 h by flow cytometry after staining (annexin-V and PI). (B) Percentage of cells found in the different regions of the histograms. (C) Images of cell morphology under the microscope.

2.2.6. Competitive inhibition of colchicine binding to tubulin

To investigate the possible binding site of **13d**, a fluorescence based competitive

assay for the colchicine site was performed. Colchicine, which does not fluoresce, exhibits marked fluorescence when bond to tubulin [44]. The changes in fluorescence intensity of colchicine could be used as an index for **13d** competition with colchicine in tubulin binding [45, 46]. As shown in Figure 6, compound **13d** decreased the fluorescence intensity of colchicine-tubulin complex in a concentration-dependent manner. Paclitaxel did not change the binding of colchicine to tubulin. These results indicated that compound **13d** binds at the colchicine site of tubulin.

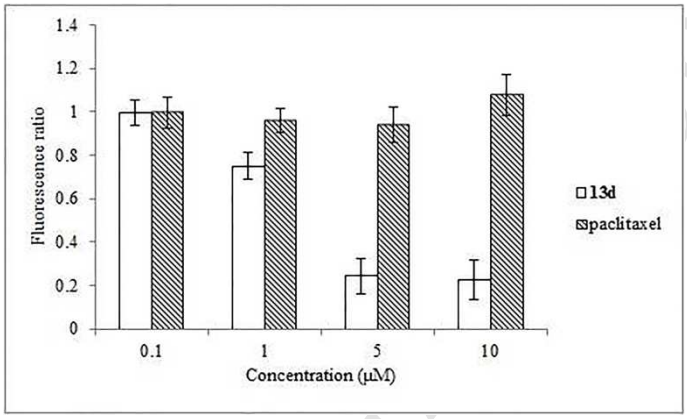

Figure 6. Fluorescence based colchicine competitive binding assay. Tubulin (4 μM) was co-incubated with indicated concentrations of paclitaxel or **13d** for 1 h, then 10 μM colchicine was added. Fluorescence values were normalized to control (DMSO).

2.3. Molecular modeling

Molecular docking was performed to study the binding mode of the most potent compound **13d**. Compound **13d** was docked into the *N*-deacetyl-*N*-(2-mercaptoacetyl) colchicine (DAMA-colchicine) binding site of the tubulin (PDB ID: 1SA0) using surflex dock program (Sybyl-X 2.1) [47]. Some of the top 20 docking poses ranked by total scores were shown in figure 7A. The binding orientation of compound **13d** was very similar to that of the cocrystallized DAMA-colchicine. As shown in figure 7B, a hydrogen bond is present between the quinoxalinone of **13d** and Thr 179 in the loop of α-tubulin. The trimethoxyphenyl moiety occupied similar conformational space as that of DAMA-colchicine and made nonpolar interaction with Cys 241, Leu 248, Ala 250, Leu 255, Ala 316 of β-tubulin.

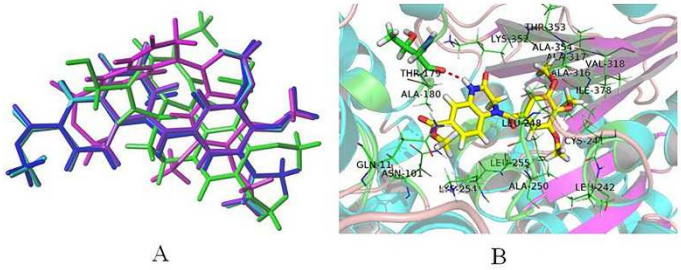

Figure 7. (A) Comparison between pose of cocrystallized DAMA-colchicine (green) with tubulin and docking poses of **13d**. (B) Proposed binding mode of **13d**. Residues within 3.5 Å of **13d** are shown.

3. Conclusion

We have synthesized a series of *N*-substituted 3-oxo-1,2,3,4-tetrahydro-quinoxaline-6-carboxylic acid derivatives with antiproliferative activity and inhibition of tubulin polymerization activity. The methyl carboxylate on the quinoxalinone was crucial for the antiproliferative activity. When this moiety was hydrolyzed to carboxylate acid or replaced with amide, the activity decreases. The replacement of benzyl group with benzoyl group led to a remarkable improvement of in vitro antiproliferative activity. This led the discovery of **13d** with IC_{50} values in the range of 0.071 to 0.164 μM against the three cancer cell lines. Immunofluorescence assay revealed that compound **13d** induced mitotic arrest in HeLa cells through disruption of microtubule dynamics. Compound **13d** induced cell cycle arrest at the G2/M phase and led to cell apoptosis. Compound **13d** represented a novel lead compound of *N*-substituted 3-oxo-1,2,3,4-tetrahydro-quinoxaline structure that paved the way for the development of new promising anticancer agents.

4. Experimental section

4.1. Chemistry

4.1.1. General

All commercially obtained reagents and solvents were used as received. Reactions were monitored by TLC with silica gel plates (0.25mm, indicator GF254, Qingdao Haiyang Co. Ltd., China) under UV light. Column chromatography was

performed with silica gel (100-200 mesh, 200-300 mesh, Qingdao Haiyang Co. Ltd., China). The melting points were measured on a hot-stage microscope (SGW X-4, Shanghai Shenguang Instrument Co. Ltd., China) and were uncorrected. Mass spectra were measured on a Bruker AmaZon SL mass spectrometer. HRMS spectra were acquired on a Thermo Scientific LTQ Orbitrap XL mass spectrometer, and all the errors were less than 3 ppm. ^{1}H NMR spectra and ^{13}C NMR spectra were acquired on a Bruker DRX 300 NMR spectrometer using $CDCl_3$ or CD_3OD as solvent (unless otherwise stated). Chemical shifts were reported in parts per million (ppm, δ) relative to the solvent peak (^{1}H, $CDCl_3$ δ 7.26 ppm, CD_3OD δ 3.31 ppm; ^{13}C, $CDCl_3$ δ 77.0 ppm, CD_3OD δ 47.6 ppm). Coupling constants (J) were measured in hertz (Hz). The infrared (IR) spectra were obtained using a Vertex 70 (Bruker, Germany) Fourier-transform infrared spectrometer.

4.1.2. Procedure for synthesis of compound 5a

The commercial compound **4** (4.50 g, 24.7 mmol) was dissolved in methanol (80 mL). The reaction was cooled to 0 ^{o}C, and thionyl chloride (5.38 mL, 74.1 mmol, 3 equiv) was added dropwise. The reaction mixture was stirred at 0 ^{o}C for 30 min and was heated to 50 ^{o}C for 4 h. The precipitate formed on cooling was collected by filtration. The solvent was removed under reduced pressure. The residue was dissolved with water and extracted with ethyl acetate. The organic layer was dried over anhydrous Na_2SO_4, and the solvent was removed by evaporation. The yellow solid was combined.

Methyl 4-amino-3-nitrobenzoate (**5a**). Yield: 89.2%, yellow solid, mp 181.9 – 182.7 ^{o}C. ^{1}H NMR (300 MHz, $CDCl_3$) δ 8.85 (d, J = 1.9 Hz, 1H), 7.99 (dd, J = 8.8, 1.9 Hz, 1H), 6.83 (d, J = 8.8 Hz, 1H), 6.42 (brs, 2H), 3.90 (s, 3H). IR (KBr) (ν_{max}/cm^{-1}): 3475, 3343, 3030, 2961, 2855, 1702, 1634, 1565, 1522, 1477, 1356, 1298, 1262, 1133, 832, 760. MS (ESI) $[M+H]^+$ 197.06.

4.1.3. General procedure for synthesis of compounds 5b-5e

To a solution of compound **4** (250 mg, 1.37 mmol) in dry CH_2Cl_2 (30 mL) were added EDCI (314 mg, 1.64 mmol, 1.2 equiv) and the amine (1.37 mmol, 1 euqiv). The reaction mixture was stirred at room temperature for 2 h. After completion of the

reaction, the mixture was washed with water and dried over anhydrous Na_2SO_4. The solvent was removed by evaporation to give the crude product, which was purified by column chromatography.

4.1.3.1. 4-Amino-*N*-butyl-3-nitrobenzamide (5b). Yield: 84.0%, yellow solid, mp 162.8 – 164.6 ^oC. ^1H NMR (300 MHz, $CDCl_3$) δ 8.47 (s, 1H), 7.90 (d, *J* = 8.7 Hz, 1H), 6.86 (d, *J* = 8.7 Hz, 1H), 6.35 (brs, 2H), 6.05 (brs, 1H), 3.42 – 3.49 (m, 2H), 1.58 – 1.67 (m, 2H), 1.35 – 1.49 (m, 2H), 0.97 (t, *J* = 7.3 Hz, 3H). IR (KBr) (ν_{max}/cm^{-1}): 3468, 3356, 3301, 2959, 2938, 2869, 1630, 1547, 1515, 1473, 1372, 1346, 840, 761. MS (ESI) $[M+H]^+$ 238.08.

4.1.3.2. 4-Amino-*N*-cyclohexyl-3-nitrobenzamide (5c). Yield: 77.9%, yellow solid, mp 205.3 – 207.6 ^oC. ^1H NMR (300 MHz, $CDCl_3$) δ 8.46 (s, 1H), 7.90 (d, *J* = 8.7 Hz, 1H), 6.86 (d, *J* = 8.7 Hz, 1H), 6.33 (brs, 2H), 5.80 – 5.93 (m, 1H), 3.89 – 4.01 (m, 1H), 1.97 – 2.08 (m, 2H), 1.73 – 1.82 (m, 2H), 1.61 – 1.71 (m, 1H), 1.35 – 1.50 (m, 2H), 1.20 – 1.30 (m, 3H). IR (KBr) (ν_{max}/cm^{-1}): 3493, 3380, 3266, 3080, 2930, 2857, 1633, 1552, 1515, 1336, 835, 759. MS (ESI) $[M-1]^-$ 262.12.

4.1.3.3. 4-Amino-3-nitro-*N*-phenylbenzamide (5d). Yield: 73.8%, yellow solid, mp 222.5 – 224.5 ^oC. ^1H NMR (300 MHz, CD_3OD) δ 8.76 (s, 1H), 7.94 (d, *J* = 9.0 Hz, 1H), 7.65 (d, *J* = 8.0 Hz, 2H), 7.35 (t, *J* = 8.0 Hz, 2H), 7.13 (t, *J* = 7.4 Hz, 1H), 7.05 (d, *J* = 9.0 Hz, 1H). IR (KBr) (ν_{max}/cm^{-1}): 3459, 3391, 3352, 1630, 1547, 1510, 1417, 1358, 827, 753. MS (ESI) $[M-1]^-$ 256.08.

4.1.3.4. (4-Amino-3-nitrophenyl)(morpholino)methanone (5e). Yield: 71.8%, yellow solid, mp 203.1 – 205.4 ^oC. ^1H NMR (300 MHz, $CDCl_3$) δ 8.24 (s, 1H), 7.51 (d, *J* = 8.6 Hz, 1H), 6.86 (d, *J* = 8.6 Hz, 1H), 6.28 (brs, 2H), 3.71 (brs, 4H), 3.67 (brs, 4H). IR (KBr) (ν_{max}/cm^{-1}): 3464, 3302, 2918, 2864, 1621, 1559, 1517, 1475, 1347, 1254, 1072, 868, 755. MS (ESI) $[M-1]^-$ 250.06.

4.1.4. General procedure for synthesis of compounds 6a-6e

A mixture of compound **5** (1.53 mmol), Cs_2CO_3 (600 mg, 1.84 mmol, 1.2 equiv) and ethyl bromoacetate (1.70 mL, 15.3 mmol, 10 equiv) was heated at 140 ^oC for 20 h. After completion of the reaction, ethyl bromoacetate was removed by evaporation. The residue was dissolved in CH_2Cl_2 and Cs_2CO_3 was removed by filtration. The

solvent was removed by evaporation to give the crude product, which was then purified by column chromatography.

4.1.4.1. Methyl 4-((2-ethoxy-2-oxoethyl)amino)-3-nitrobenzoate (6a). Yield: 58.3%, light yellow solid, mp 127.6 – 128.8 ^{o}C. ^{1}H NMR (300 MHz, $CDCl_3$) δ 8.91 (d, *J* = 2.1 Hz, 1H), 8.75 (brs, 1H), 8.09 (dd, *J* = 9.0, 2.1 Hz, 1H), 6.72 (d, *J* = 9.0 Hz, 1H), 4.31 (q, *J* = 7.2 Hz, 2H), 4.14 (d, *J* = 5.2 Hz, 2H), 3.91 (s, 3H), 1.33 (t, *J* = 7.2 Hz, 3H). IR (KBr) (ν_{max}/cm^{-1}): 3345, 3098, 2985, 2955, 2851, 1740, 1708, 1628, 1570, 1532, 1438, 1373, 1162, 1132, 827, 763. MS (ESI) $[M+H]^+$ 283.09.

4.1.4.2. Ethyl 2-((4-(butylcarbamoyl)-2-nitrophenyl)amino)acetate (6b). Yield: 46.2%, light yellow solid, mp 152.8 – 154.0 ^{o}C. ^{1}H NMR (300 MHz, $CDCl_3$) δ 8.66 (brs, 1H), 8.55 (s, 1H), 8.01 (d, *J* = 8.7 Hz, 1H), 6.76 (d, *J* = 8.7 Hz, 1H), 6.05 (brs, 1H), 4.31 (q, *J* = 7.2 Hz, 2H), 4.13 (d, *J* = 5.1 Hz, 2H), 3.40 – 3.51 (m, 2H), 1.57 – 1.67 (m, 2H), 1.37 – 1.49 (m, 2H), 1.33 (t, *J* = 7.2 Hz, 3H), 0.97 (t, *J* = 7.2 Hz, 3H). IR (KBr) (ν_{max}/cm^{-1}): 3338, 3277, 3095, 2924, 2861, 1726, 1633, 1554, 1524, 1446, 1369, 1253, 1066, 1018, 835, 732. MS (ESI) $[M-1]^-$ 322.41.

4.1.4.3. Ethyl 2-((4-(cyclohexylcarbamoyl)-2-nitrophenyl)amino)acetate (6c). Yield: 45.6%, light yellow solid, mp 173.5 – 175.0 ^{o}C. ^{1}H NMR (300 MHz, $CDCl_3$) δ 8.66 (brs, 1H), 8.53 (s, 1H), 8.00 (d, *J* = 8.7 Hz, 1H), 6.75 (d, *J* = 8.7 Hz, 1H), 5.90 (d, *J* = 7.7 Hz, 1H), 4.31 (q, *J* = 7.2 Hz, 2H), 4.13 (d, *J* = 5.2 Hz, 2H), 3.90 – 4.01 (m, 1H), 1.99 – 2.07 (m, 2H), 1.73 – 1.82 (m, 2H), 1.63 – 1.71 (m, 1H), 1.39 – 1.51 (m, 2H), 1.23 – 1.33 (m, 6H). IR (KBr) (ν_{max}/cm^{-1}): 3425, 3355, 3283, 3085, 2930, 2857, 1741, 1630, 1524, 1369, 1232, 1072, 829, 758. MS (ESI) $[M-1]^-$ 348.44.

4.1.4.4. Ethyl 2-((2-nitro-4-(phenylcarbamoyl)phenyl)amino)acetate (6d). Yield: 46.5%, light yellow solid, mp 187.2 – 189.0 ^{o}C. ^{1}H NMR (300 MHz, $CDCl_3$) δ 8.74 (brs, 1H), 8.71 (s, 1H), 8.09 (d, *J* = 8.7 Hz, 1H), 7.76 (brs, 1H), 7.64 (d, *J* = 7.5 Hz, 2H), 7.39 (t, *J* = 7.5 Hz, 2H), 7.17 (t, *J* = 7.5 Hz, 1H), 6.82 (d, *J* = 8.7 Hz, 1H), 4.32 (q, *J* = 7.2 Hz, 2H), 4.16 (d, *J* = 5.2 Hz, 2H), 1.34 (t, *J* = 7.2 Hz, 3H). IR (KBr) (ν_{max}/cm^{-1}): 3389, 3337, 3283, 3062, 2922, 2854, 1730, 1637, 1522, 1440, 1391, 1320, 1247, 1068, 828, 754. MS (ESI) $[M-1]^-$ 342.28.

4.1.4.5. Ethyl 2-((4-(morpholine-4-carbonyl)-2-nitrophenyl)amino)acetate (6e).

Yield: 44.3%, light yellow solid, mp 78.5 – 80.7 ^{o}C. ^{1}H NMR (300 MHz, $CDCl_3$) δ 8.59 (brs, 1H), 8.33 (s, 1H), 7.62 (d, *J* = 8.7 Hz, 1H), 6.75 (d, *J* = 8.7 Hz, 1H), 4.31 (q, *J* = 7.2 Hz, 2H), 4.12 (d, *J* = 5.2 Hz, 2H), 3.71 (brs, 4H), 3.67 (brs, 4H), 1.33 (t, *J* = 7.2 Hz, 3H). IR (KBr) (ν_{max}/cm^{-1}): 3441, 3369, 3108, 2976, 2920, 2857, 1741, 1633, 1564, 1530, 1456, 1355, 1227, 1067, 823, 755. MS (ESI) $[M-1]^-$ 336.54.

4.1.5. General procedure for synthesis of compounds 7a-7e

To a solution of compound **6** in methanol was added palladium-carbon catalyst (10%, 0.05 equip). The reactor was purged with hydrogen. The reaction was carried out under a hydrogen atmosphere at room temperature for 12 h. The palladium-carbon was removed by suction filtration and the solvent was removed under reduced pressure. The crude product was purified by column chromatography.

4.1.5.1. Methyl 3-oxo-1,2,3,4-tetrahydroquinoxaline-6-carboxylate (7a). Yield: 82.4%, gray solid, mp > 280 ^{o}C. ^{1}H NMR (300 MHz, $CDCl_3$) δ 7.74 (brs, 1H), 7.60 (d, *J* = 8.4 Hz, 1H), 7.38 (s, 1H), 6.64 (d, *J* = 8.4 Hz, 1H), 4.09 (s, 2H), 3.87 (s, 3H). IR (KBr) (ν_{max}/cm^{-1}): 3317, 3254, 3104, 3040, 2953, 2847, 1672, 1610, 1550, 1504, 1444, 1398, 1295, 1222, 1111, 821, 771. MS (ESI) $[M+H]^+$ 207.00.

4.1.5.2. *N*-butyl-3-oxo-1,2,3,4-tetrahydroquinoxaline-6-carboxamide (7b). Yield: 68.8%, gray solid, mp 211.9 – 213.3 ^{o}C. ^{1}H NMR (300 MHz, CD_3OD) δ 7.32 (d, *J* = 8.1 Hz, 1H), 7.24 (s, 1H), 6.67 (d, *J* = 8.1 Hz, 1H), 3.92 (s, 2H), 3.32 – 3.37 (m, 2H), 1.54 – 1.63 (m, 2H), 1.35 – 1.44 (m, 2H), 0.96 (t, *J* = 7.2 Hz, 3H). IR (KBr) (ν_{max}/cm^{-1}): 3340, 3096, 2963, 2873, 1696, 1602, 1521, 1456, 1389, 819, 762. MS (ESI) $[M-1]^-$ 246.44.

4.1.5.3. *N*-cyclohexyl-3-oxo-1,2,3,4-tetrahydroquinoxaline-6-carboxamide (7c). Yield: 71.3%, gray solid, mp 268.8 – 270.8 ^{o}C. ^{1}H NMR (300 MHz, $CDCl_3$) δ 7.61 (s, 1H), 7.21 (d, *J* = 8.1 Hz, 1H), 6.64 (d, *J* = 8.1 Hz, 1H), 5.79 (brs, 1H), 4.05 (s, 2H), 3.91 – 3.99 (m, 1H), 1.99 – 2.06 (m, 2H), 1.70 – 1.80 (m, 2H), 1.62 – 1.67 (m, 1H), 1.40 – 1.47 (m, 2H), 1.18 – 1.24 (m, 3H). IR (KBr) (ν_{max}/cm^{-1}): 3392, 3291, 2929, 2854, 1678, 1634, 1541, 1454. MS (ESI) $[M-1]^-$ 272.22.

4.1.5.4. 3-Oxo-*N*-phenyl-1,2,3,4-tetrahydroquinoxaline-6-carboxamide (7d). Yield: 74.9%, gray solid, mp 260.9 – 262.5 ^{o}C. ^{1}H NMR (300 MHz, CD_3OD) δ 7.62

(d, *J* = 7.5 Hz, 2H), 7.49 (d, *J* = 8.1 Hz, 1H), 7.36 (s, 1H), 7.33 (t, *J* = 7.5, 2H), 7.11 (t, *J* = 7.2 Hz, 1H), 6.73 (d, *J* = 8.1 Hz, 1H), 3.95 (s, 2H). IR (KBr) (ν_{max}/cm^{-1}): 3389, 2923, 2852, 1654, 1531, 1501, 820, 755. MS (ESI) $[M-1]^-$ 266.17.

4.1.5.5. 7-(Morpholine-4-carbonyl)-3,4-dihydroquinoxalin-2(1*H*)-one (7e). Yield: 70.2%, gray solid, mp 207.6 – 209.5 ^oC. ^1H NMR (300 MHz, $CDCl_3$) δ 7.85 (brs, 1H), 6.95 (d, *J* = 8.1 Hz, 1H), 6.88 (s, 1H), 6.64 (d, *J* = 8.1 Hz, 1H), 4.06 (brs, 1H), 4.03 (s, 2H), 3.69 (brs, 4H), 3.66 (brs, 4H). IR (KBr) (ν_{max}/cm^{-1}): 3279, 3209, 3041, 2966, 2923, 2857, 1679, 1612, 1499, 1274, 832, 770. MS (ESI) $[M-1]^-$ 260.14.

4.1.6. General procedure for synthesis of compounds 8a-8c

To a solution of compound **7** (30 mg, 0.145 mmol) in acetonitrile (2 mL) were added anhydrous K_2CO_3 (24 mg, 0.174 mmol, 1.2 equiv), KI (12 mg, 0.073 mmol, 0.5 equiv) and substituted benzyl chloride (0.218 mmol, 1.5 equiv). The reaction mixture was stirred at 70 ^oC for 6 h. After completion of the reaction, the mixture was filtered and the solvent was removed by evaporation to give the crude product, which was then purified by column chromatography.

4.1.6.1. Methyl 1-(4-methoxybenzyl)-3-oxo-1,2,3,4-tetrahydroquinoxaline-6-carboxylate (8a). Yield: 42.3%, white solid, mp 217.0 – 219.0 ^oC. ^1H NMR (300 MHz, $CDCl_3$) δ 8.48 (brs, 1H), 7.65 (d, *J* = 8.4 Hz, 1H), 7.44 (s, 1H), 7.19 (d, *J* = 8.1 Hz, 2H), 6.88 (d, *J* = 8.1 Hz, 2H), 6.76 (d, *J* = 8.4 Hz, 1H), 4.44 (s, 2H), 3.92 (s, 2H), 3.87 (s, 3H), 3.80 (s, 3H). ^{13}C NMR (75 MHz, $CDCl_3$) δ 166.7, 165.5, 159.3, 138.8, 128.8, 127.1, 126.7, 125.0, 119.9, 116.6, 114.4, 110.9, 55.4, 52.8, 51.9, 51.6. IR (KBr) (ν_{max}/cm^{-1}): 3429, 3288, 3073, 2924, 2844, 1709, 1679, 1613, 1504, 1438, 1383, 1295, 1225, 1171, 1037, 816, 762. HRMS (ESI): calcd for $C_{18}H_{19}N_2O_4$ $[M+H]^+$ 327.13393, found 327.13388.

4.1.6.2. Methyl 1-(3,4-dimethoxybenzyl)-3-oxo-1,2,3,4-tetrahydroquinoxaline-6-carboxylate (8b). Yield: 56.1%, white solid, mp 155.9 – 157.5 ^oC. ^1H NMR (300 MHz, $CDCl_3$) δ 9.05 (brs, 1H), 7.65 (dd, *J* = 8.7, 1.8 Hz, 1H), 7.50 (d, *J* = 1.8 Hz, 1H), 6.82 – 6.79 (m, 4H), 4.43 (s, 2H), 3.92 (s, 2H), 3.87 (s, 6H), 3.83 (s, 3H).^{13}C NMR (75 MHz, $CDCl_3$) δ 166.8, 165.8, 149.5, 148.7, 138.9, 127.6, 126.6, 125.2, 120.0, 119.9, 116.8, 111.4, 110.9, 110.5, 56.0, 53.2, 52.0, 51.6. IR (KBr) (ν_{max}/cm^{-1}): 3429,

3288, 2951, 2842, 1700, 1615, 1511, 1302, 1263, 1225, 1142, 1025, 811, 764. HRMS (ESI): calcd for $C_{19}H_{21}N_2O_5$ $[M+H]^+$ 357.14450, found 357.14450.

4.1.6.3. Methyl 3-oxo-1-(3,4,5-trimethoxybenzyl)-1,2,3,4-tetrahydroquinoxaline -6-carboxylate (8c). Yield 67.8%, white solid, mp 188.9 – 191.0 ^oC. ^1H NMR (300 MHz, $CDCl_3$) δ 8.02 (brs, 1H), 7.67 (dd, *J* = 8.4, 1.8 Hz, 1H), 7.43 (d, *J* = 1.8 Hz, 1H), 6.78 (d, *J* = 8.4 Hz, 1H), 6.47 (s, 2H), 4.42 (s, 2H), 3.93 (s, 2H), 3.88 (s, 3H), 3.84 (s, 3H), 3.81 (s, 6H). ^{13}C NMR (75 MHz, $CDCl_3$) δ 166.7, 165.7, 153.8, 138.8, 137.5, 131.0, 126.7, 125.1, 120.2, 116.8, 111.0, 104.3, 60.9, 56.2, 53.8, 52.0, 51.8. IR (KBr) (ν_{max}/cm^{-1}): 3429, 3266, 2948, 2839, 1696, 1613, 1503, 1459, 1302, 1220, 1162, 1124, 1005, 821, 766. HRMS (ESI): calcd for $C_{20}H_{23}N_2O_6$ $[M+H]^+$ 387.15506, found 387.15512.

4.1.7. Procedure for synthesis of compound 9

To a solution of compound **8c** (30 mg, 0.0776 mmol) in THF (2 mL)/H_2O (1 mL) was added anhydrous LiOH (3.7 mg, 0.155 mmol, 2 equiv). The reaction mixture was stirred at 40 ^oC for 10 h. The THF was removed by evaporation and the remaining mixture was acidified with hydrochloric acid. The precipitate that formed on cooling was collected by filtration without further purification.

3-Oxo-1-(3,4,5-trimethoxybenzyl)-1,2,3,4-tetrahydroquinoxaline-6-carboxylic acid (9). Yield: 72.6%, white solid, mp 135.3 – 136.3 ^oC. ^1H NMR (300 MHz, $CDCl_3$) δ 11.95 (brs, 1H), 7.73 (s, 1H), 7.51 (d, *J* = 8.4 Hz, 1H), 6.67 (d, *J* = 8.4 Hz, 1H), 6.51 (s, 2H), 4.46 (s, 2H), 4.04 (s, 2H), 3.84 (s, 9H). ^{13}C NMR (75 MHz, $CDCl_3$) δ 170.3, 167.8, 153.8, 138.9, 137.5, 131.0, 127.2, 124.4, 119.0, 118.6, 109.9, 104.1, 60.9, 56.3, 53.9, 51.3. IR (KBr) (ν_{max}/cm^{-1}): 3421, 3067, 2937, 2843, 1690, 1609, 1501, 1459, 1232, 1126, 820, 772. HRMS (ESI): calcd for $C_{19}H_{21}N_2O_6$ $[M+H]^+$ 373.13941, found 373.13940.

4.1.8. General procedure for synthesis of compounds 10a, 10b

To a solution of compound **9** (25mg, 0.0671 mmol) in toluene (3 mL) was added oxalyl chloride (57 μL, 0.671 mmol, 10 equiv). The reaction mixture was then stirred at 70 ^oC for 3 h. After completion of the reaction, toluene and the remaining oxalyl chloride were removed by evaporation to give the crude product without further

purification. To a solution of amine in anhydrous THF (1 mL) was added anhydrous K_2CO_3 (28 mg, 0.201 mmol, 3 equiv). A mixture of the acyl chloride prepared in the above step in anhydrous THF (1 mL) was added to the reaction mixture dropwise. The mixture was stirred at room temperature for 20 min. After completion of the reaction, the mixture was filtered and the solvent was removed by evaporation to give the crude product, which was then purified by column chromatography.

4.1.8.1. *N*-butyl-3-oxo-1-(3,4,5-trimethoxybenzyl)-1,2,3,4-tetrahydroquinoxaline -6-carboxamide (10a). Yield 73.2%, white solid, mp 184.5 – 186.0 ^{o}C. ^{1}H NMR (300 MHz, $CDCl_3$) δ 8.72 (brs, 1H), 7.52 (s, 1H), 7.24 (d, *J* = 8.4 Hz, 1H), 6.72 (d, *J* = 8.4 Hz, 1H), 6.48 (s, 2H), 6.06 (brs, 1H), 4.39 (s, 2H), 3.90 (s, 2H), 3.84 (s, 3H), 3.81 (s, 6H), 3.44 – 3.51 (m, 2H), 1.55 – 1.62 (m, 2H), 1.37 – 1.47 (m, 2H), 0.95 (t, *J* = 7.2 Hz, 3H).^{13}C NMR (75 MHz, $CDCl_3$) δ 166.6, 165.6, 153.7, 137.7, 137.5, 131.3, 126.0, 124.9, 122.2, 115.3, 111.1, 104.3, 60.9, 56.2, 53.9, 52.0, 39.9, 31.8, 20.2, 13.8. IR (KBr) (ν_{max}/cm^{-1}): 3377, 3225, 3074, 2930, 2863, 1693, 1619, 1510, 1459, 1235, 1181, 1127, 817, 767. HRMS (ESI): calcd for $C_{23}H_{30}N_3O_5$ $[M+H]^+$ 428.21800, found 428.21802.

4.1.8.2. *N*-cyclohexyl-3-oxo-1-(3,4,5-trimethoxybenzyl)-1,2,3,4-tetrahydroquinoxa line-6-carboxamide (10b). Yield: 62.4%, white solid, mp 167.1 – 169.0 ^{o}C. ^{1}H NMR (300 MHz, $CDCl_3$) δ 8.80 (brs, 1H), 7.55 (d, *J* = 1.5 Hz, 1H), 7.24 (dd, *J* = 8.4, 1.5 Hz, 1H), 6.70 (d, *J* = 8.4 Hz, 1H), 6.48 (s, 2H), 5.91 (d, *J* = 8.1 Hz, 1H), 4.39 (s, 2H), 4.01 – 4.07 (m, 1H), 3.90 (s, 2H), 3.84 (s, 3H), 3.81 (s, 6H), 1.95 – 2.08 (m, 2H), 1.68 – 1.80 (m, 3H), 1.39 – 1.50 (m, 2H), 1.15 – 1.23 (m, 3H). ^{13}C NMR (75 MHz, $CDCl_3$) δ 165.7, 165.6, 153.7, 137.6, 137.5, 131.3, 126.1, 125.1, 122.1, 115.5, 111.0, 104.3, 60.9, 56.2, 53.9, 52.1, 48.7, 33.4, 25.6, 24.9. IR (KBr) (ν_{max}/cm^{-1}): 3425, 2931, 2854, 1689, 1620, 1508, 1458, 1383, 1231, 1126, 822, 765. HRMS (ESI): calcd for $C_{25}H_{32}N_3O_5$ $[M+H]^+$ 454.23365, found 454.23367.

4.1.9. General procedure for synthesis of compounds 12a-12e

A mixture of substituted benzoic acids and thionyl chloride (15 equiv) was heated at 70 ^{o}C for 3 h. After completion of the reaction, remaining thionyl chloride was removed by evaporation to give the crude product without further purification.

4.1.10. General procedure for synthesis of compounds 13a-13l

To a solution of compound **7** in anhydrous THF (1 mL) was added anhydrous K_2CO_3 (2 equiv). A mixture of the acyl chloride (2 equiv) prepared in the above step in anhydrous THF (1 mL) was added to the reaction mixture dropwise. The mixture was stirred at room temperature for 20 h. After completion of the reaction, the mixture was filtered and the solvent was removed by evaporation to give the crude product, which was then purified by column chromatography.

4.1.10.1. Methyl 1-(4-fluorobenzoyl)-3-oxo-1,2,3,4-tetrahydroquinoxaline-6-carboxylate (13a). Yield: 59.7 %, white solid, mp 239.6 – 241.5 ^{o}C. ^{1}H NMR (300 MHz, $CDCl_3$) δ 9.31 (brs, 1H), 7.71 (d, *J* = 1.2 Hz, 1H), 7.39 – 7.53 (m, 3H), 7.02 (t, *J* = 8.4 Hz, 2H), 6.70 (d, *J* = 8.4 Hz, 1H), 4.60 (s, 2H), 3.91 (s, 3H). ^{13}C NMR (75 MHz, $CDCl_3$) δ 168.2, 167.9, 165.9, 164.5 (*J* = 252), 131.4 (*J* = 8.25), 131.5, 129.9, 129.6 (*J* = 3.75), 127.8, 124.3, 124.2, 117.9, 115.9 (*J* = 21.7), 52.5, 47.6. IR (KBr) (ν_{max}/cm^{-1}): 3422, 3074, 2957, 2925, 2857, 1713, 1664, 1606, 1497, 1440, 1347, 1296, 1231, 1153, 806, 763. HRMS (ESI): calcd for $C_{17}H_{14}FN_2O_4$ $[M+H]^+$ 329.09321, found 329.09311.

4.1.10.2. Methyl 1-(4-methoxybenzoyl)-3-oxo-1,2,3,4-tetrahydroquinoxaline -6-carboxylate (13b). Yield: 58.3 %, white solid, mp 205.5 – 207.2 ^{o}C. ^{1}H NMR (300 MHz, $CDCl_3$) δ 9.37 (brs, 1H), 7.70 (d, *J* = 1.8 Hz, 1H), 7.46 (dd, *J* = 8.4, 1.8 Hz, 1H), 7.39 (d, *J* = 8.7 Hz, 2H), 6.81 (d, *J* = 8.7 Hz, 2H), 6.73 (d, *J* = 8.4 Hz, 1H), 4.59 (s, 2H), 3.90 (s, 3H), 3.82 (s, 3H). ^{13}C NMR (75 MHz, $CDCl_3$) δ 169.0, 168.2, 166.0, 162.3, 132.2, 131.3, 129.7, 127.3, 125.4, 124.3, 124.2, 117.8, 113.8, 55.4, 52.5, 47.7. IR (KBr) (ν_{max}/cm^{-1}): 3431, 2924, 2852, 1711, 1664, 1607, 1498, 1440, 1345, 1296, 1245, 1168, 906, 843, 764. HRMS (ESI): calcd for $C_{18}H_{17}N_2O_5$ $[M+H]^+$ 341.11320, found 341.11310.

4.1.10.3. Methyl 1-(3,4-dimethoxybenzoyl)-3-oxo-1,2,3,4-tetrahydro quinoxaline-6-carboxylate (13c). Yield: 46.7 %, white solid, mp 217.0 – 218.8 ^{o}C. ^{1}H NMR (300 MHz, $CDCl_3$) δ 9.39 (brs, 1H), 7.70 (d, *J* = 1.8 Hz, 1H), 7.47 (dd, *J* = 8.4, 1.8 Hz, 1H), 7.04 (d, *J* = 1.8 Hz, 1H), 6.95 (dd, *J* = 8.4, 1.8 Hz, 1H), 6.75 (d, *J* = 8.4 Hz, 1H), 6.70 (d, *J* = 8.4 Hz, 1H), 4.59 (s, 2H), 3.90 (s, 3H), 3.88 (s, 3H), 3.78 (s,

3H). ^{13}C NMR (75 MHz, $CDCl_3$) δ 169.0, 168.1, 166.0, 152.0, 148.9, 132.2, 129.6, 127.3, 125.4, 124.3, 124.2, 123.1, 117.8, 112.2, 110.3, 56.0, 52.5, 47.8. IR (KBr) (ν_{max}/cm^{-1}): 3430, 3070, 2923, 2854, 1705, 1601, 1510, 1362, 1297, 1273, 1220, 1143, 824, 763. HRMS (ESI): calcd for $C_{19}H_{19}N_2O_6$ $[M+H]^+$ 371.12376, found 371.12363.

4.1.10.4. Methyl 3-oxo-1-(3,4,5-trimethoxybenzoyl)-1,2,3,4-tetrahydroquinoxaline-6-carboxylate (13d). Yield 58.5 %, white solid, mp 92.0 – 94.6 ^{o}C. ^{1}H NMR (300 MHz, $CDCl_3$) δ 8.99 (brs, 1H), 7.67 (s, 1H), 7.51 (d, *J* = 8.1 Hz, 1H), 6.83 (d, *J* = 8.1 Hz, 1H), 6.64 (s, 2H), 4.59 (s, 2H), 3.91 (s, 3H), 3.87 (s, 3H), 3.70 (s, 6H). ^{13}C NMR (75 MHz, $CDCl_3$) δ 168.9, 167.7, 165.9, 153.1, 141.0, 131.7, 129.6, 128.2, 127.5, 124.3, (2C) 117.6, 106.5, 61.1, 56.2, 52.5, 47.8. IR (KBr) (ν_{max}/cm^{-1}): 3429, 2927, 2853, 1705, 1591, 1494, 1422, 1353, 1298, 1221, 1124, 847, 763. HRMS (ESI): calcd for $C_{20}H_{21}N_2O_7$ $[M+H]^+$ 401.13433, found 401.13437.

4.1.10.5. Methyl 3-oxo-1-(2-(3,4,5-trimethoxyphenyl)acetyl)-1,2,3,4-tetrahydroquinoxaline-6-carboxylate (13e). Yield: 63.2 %, white solid, mp 188.0 – 181.9 ^{o}C. ^{1}H NMR (300 MHz, CD_3OD) δ 7.75 (d, *J* = 8.4 Hz, 1H), 7.67 (d, *J* = 8.4 Hz, 1H), 7.51 (s, 1H), 6.26 (s, 2H), 4.45 (s, 2H), 3.92 (s, 2H), 3.90 (s, 3H), 3.71 (s, 6H), 3.68 (s, 3H). ^{13}C NMR (75 MHz, $CDCl_3$) δ 170.4, 165.8, 153.4, 137.0, 130.8, 129.3, 128.7, 124.6, 124.2 (2C), 117.9, 106.4, 105.6, 60.9, 56.1, 52.6, 41.4, 41.1. IR (KBr) (ν_{max}/cm^{-1}): 3430, 3069, 2929, 2846, 1682, 1596, 1498, 1432, 1373, 1303, 1234, 1190, 1123, 831, 769. HRMS (ESI): calcd for $C_{21}H_{23}N_2O_7$ $[M+H]^+$ 415.14998, found 415.14999.

4.1.10.6. *N*-butyl-1-(3,4-dimethoxybenzoyl)-3-oxo-1,2,3,4-tetrahydro quinoxaline-6-carboxamide (13f). Yield: 55.1 %, white solid, mp 224.5-226.7 ^{o}C. ^{1}H NMR (300 MHz, CD_3OD) δ 7.50 (s, 1H), 7.20 (d, *J* = 8.4 Hz, 1H), 6.95 – 7.02 (m, 2H), 6.89 (d, *J* = 8.7 Hz, 1H), 6.79 (d, *J* = 8.4 Hz, 1H), 4.50 (s, 2H), 3.82 (s, 3H), 3.69 (s, 3H), 3.31 – 3.39 (m, 2H), 1.51 – 1.63 (m, 2H), 1.34 – 1.42 (m, 2H), 0.95 (t, *J* = 7.2 Hz, 3H). ^{13}C NMR (75 MHz, CD_3OD) δ 169.5, 168.1, 167.4, 152.0, 148.8, 132.1, 130.9, 130.4, 125.8, 124.0, 122.7, 120.5, 115.6, 112.2, 110.6, 55.0 (2C), 39.4, 31.2, 19.8, 12.8. IR (KBr) (ν_{max}/cm^{-1}): 3413, 3076, 2928, 2865, 1696, 1652, 1595, 1549, 1511, 1364, 1267, 1222, 1140, 826, 760. HRMS (ESI): calcd for $C_{22}H_{26}N_3O_5$ $[M+H]^+$

412.18670, found 412.18668.

4.1.10.7. *N*-butyl-3-oxo-1-(3,4,5-trimethoxybenzoyl)-1,2,3,4-tetrahydro quinoxaline-6-carboxamide (13g). Yield: 65.3 %, white solid, mp 230.5 – 232.0 ^{o}C. ^{1}H NMR (300 MHz, CD_3OD) δ 7.50 (s, 1H), 7.23 (d, *J* = 8.4 Hz, 1H), 6.86 (d, *J* = 8.4 Hz, 1H), 6.70 (s, 2H), 4.51 (s, 2H), 3.77 (s, 3H), 3.69 (s, 6H), 3.32 – 3.37 (m, 2H), 1.52 – 1.62 (m, 2H), 1.34 – 1.44 (m, 2H), 0.95 (t, *J* = 7.3 Hz, 3H). ^{13}C NMR (75 MHz, MeOD) δ 169.4, 167.9, 167.4, 153.1, 140.5, 132.3, 131.0, 130.1, 129.0, 124.1, 120.5, 115.5, 106.3, 59.8, 55.2, 39.4, 31.2, 19.8, 12.7. IR (KBr) (ν_{max}/cm^{-1}): 3428, 2939, 2868, 1695, 1636, 1587, 1420, 1361, 1239, 1129, 845, 758. HRMS (ESI): calcd for $C_{23}H_{28}N_3O_6$ $[M+H]^+$ 442.19726, found 442.19727.

4.1.10.8. *N*-cyclohexyl-3-oxo-1-(3,4,5-trimethoxybenzoyl)-1,2,3,4-tetrahydro quinoxaline-6-carboxamide (13h). Yield: 54.6 %, white solid, mp 263.9 – 264.9 ^{o}C. ^{1}H NMR (300 MHz, $CDCl_3$) δ 9.07 (brs, 1H), 7.84 (s, 1H), 7.07 (d, *J* = 8.4 Hz, 1H), 6.83 (d, *J* = 8.4 Hz, 1H), 6.66 (s, 2H), 5.98 (d, *J* = 8.1 Hz, 1H), 4.56 (s, 2H), 4.01 – 4.10 (m, 1H), 3.88 (s, 3H), 3.73 (s, 6H), 1.99 – 2.08 (m, 2H), 1.64 – 1.80 (m, 3H), 1.24 – 1.53 (m, 2H), 1.25 – 1.29 (m, 3H). ^{13}C NMR (75 MHz, $CDCl_3$) δ 169.0, 167.0, 164.9, 153.2, 140.8, 132.0, 130.6, 130.2, 128.6, 124.0, 119.8, 116.8, 106.4, 61.0, 56.3, 49.1, 48.1, 33.2, 25.5, 24.8. IR (KBr) (ν_{max}/cm^{-1}): 3384, 3281, 2931, 2856, 1692, 1642, 1587, 1502, 1459, 1361, 1214, 1129, 1000, 843, 759. HRMS (ESI): calcd for $C_{25}H_{30}N_3O_6$ $[M+H]^+$ 468.21291, found 468.21289.

4.1.10.9. 1-(3,4-Dimethoxybenzoyl)-3-oxo-*N*-phenyl-1,2,3,4-tetrahydro quinoxaline-6-carboxamide (13i). Yield: 51.5 %, white solid, mp 274.7 – 276.5 ^{o}C. ^{1}H NMR (300 MHz, $CDCl_3$) δ 8.25 (brs, 1H), 7.75 (brs, 1H), 7.56 – 7.65 (m, 3H), 7.38 (t, *J* = 7.5 Hz, 2H), 7.15 – 7.25 (m, 2H), 7.07 (s, 1H), 6.97 (d, *J* = 8.4 Hz, 1H), 6.85 (d, *J* = 8.4 Hz, 1H), 6.76 (d, *J* = 8.1 Hz, 1H), 4.58 (s, 2H), 3.90 (s, 3H), 3.82 (s, 3H). ^{13}C NMR (75 MHz, $CDCl_3$) δ 167.2, 164.0 (2C), 152.0, 149.0, 137.5, 131.2, 129.2, 125.5 (2C), 125.0 (2C), 124.4, 123.0, 120.6, 120.2, 116.0, 112.1, 110.3, 56.0, 48.0. IR (KBr) (ν_{max}/cm^{-1}): 3426, 3297, 3073, 2924, 2854, 1691, 1658, 1595, 1513, 1445, 1369, 1328, 1267, 1142, 824, 759. HRMS (ESI): calcd for $C_{24}H_{22}N_3O_5$ $[M+H]^+$ 432.15540, found 432.15540.

4.1.10.10. 3-Oxo-*N*-phenyl-1-(3,4,5-trimethoxybenzoyl)-1,2,3,4-tetrahydro quinoxaline-6-carboxamide (13j). Yield: 55.3 %, white solid, mp 247.1 – 248.5 ^{o}C. ^{1}H NMR (300 MHz, $CDCl_3$) δ 9.11 (brs, 1H), 8.07 (brs, 1H), 7.61 – 7.66 (m, 3H), 7.36 (t, *J* = 7.5 Hz, 2H), 7.27 (s, 1H), 7.15 (t, *J* = 7.5 Hz, 1H), 6.93 (d, *J* = 8.4 Hz, 1H), 6.67 (s, 2H), 4.53 (s, 2H), 3.88 (s, 3H), 3.73 (s, 6H). ^{13}C NMR (75 MHz, $CDCl_3$) δ 169.2, 167.3, 164.2, 153.2, 140.9, 137.6, 132.3, 130.5, 130.4, 129.2, 128.4, 125.0, 124.3, 120.8, 120.4, 116.3, 106.4, 61.0, 56.3, 48.2. IR (KBr) (ν_{max}/cm^{-1}): 3296, 3065, 2935, 2866, 1690, 1591, 1502, 1446, 1364, 1332, 1238, 1210, 1126, 824, 759. HRMS (ESI): calcd for $C_{25}H_{24}N_3O_6$ $[M+H]^+$ 462.16596, found 462.16595.

4.1.10.11. 4-(3,4-dimethoxybenzoyl)-7-(morpholine-4-carbonyl)-3,4-dihydro quinoxalin-2(1*H*)-one (13k). Yield: 50.3 %, white solid, mp 204.0 – 205.1 ^{o}C. ^{1}H NMR (300 MHz, $CDCl_3$) δ 8.62 (brs, 1H), 7.11 (d, *J* = 13.8 Hz, 2H), 6.94 (d, *J* = 8.4 Hz, 1H), 6.83 (s, 2H), 6.74 (d, *J* = 8.4 Hz, 1H), 4.55 (s, 2H), 3.89 (s, 3H), 3.83 (s, 3H), 3.69 (brs, 4H), 3.54 – 3.58 (m, 4H).^{13}C NMR (75 MHz, $CDCl_3$) δ 169.0 (2C), 167.5, 151.9, 149.0, 132.5, 130.2, 129.6, 125.5, 124.2, 122.9, 121.6, 116.1, 112.1, 110.3, 66.8, 56.0 (2C), 48.1. IR (KBr) (ν_{max}/cm^{-1}): 3350, 3071, 2923, 2856, 1705, 1642, 1514, 1472, 1343, 1268, 1226, 1139, 1111, 1023, 764, 728. HRMS (ESI): calcd for $C_{22}H_{24}N_3O_6$ $[M+H]^+$ 426.16596, found 426.16595.

4.1.10.12. 7-(Morpholine-4-carbonyl)-4-(3,4,5-trimethoxybenzoyl)-3,4-dihydro quinoxalin-2(1*H*)-one (13l). Yield 53.3 %, white solid, mp 205.5 – 207.0 ^{o}C. ^{1}H NMR (300 MHz, $CDCl_3$) δ 8.86 (brs, 1H), 7.16 (s, 1H), 6.94 (d, *J* = 8.4 Hz, 1H), 6.88 (d, *J* = 8.4 Hz, 1H), 6.66 (s, 2H), 4.54 (s, 2H), 3.87 (s, 3H), 3.74 (s, 6H), 3.69 (brs, 4H), 3.50 – 3.61 (m, 4H). ^{13}C NMR (75 MHz, $CDCl_3$) δ 169.0, 168.8, 167.4, 153.2, 141.0, 132.8, 130.4, 129.0, 128.4, 124.3, 121.5, 116.1, 106.4, 66.8, 61.0, 56.3, 48.3. IR (KBr) (ν_{max}/cm^{-1}): 3429, 3075, 2924, 2855, 1707, 1666, 1588, 1521, 1464, 1352, 1243, 1141, 837, 782. HRMS (ESI): calcd for $C_{23}H_{26}N_3O_7$ $[M+H]^+$ 456.17653, found 456.17651.

4.2. Biological evaluation

4.2.1. Cell lines and culture conditions

The human epithelial cervical cancer cell line HeLa, the human hepatoma cell

line SMMC-7721 and the human leukemia cell line K562 were cultured in RPMI 1640 medium (HyClone Co., USA), supplemented with 10% fetal bovine serum (Sijiqing Biotechnology Co., China), in 5% CO_2 humidified air at 37 ^{o}C. All the cell lines were obtained from the American Type Culture Collection (ATCC, USA).

4.2.2. In vitro anti-proliferative activity

The in vitro anti-proliferative activities were determined with an MTT assay. Compounds were dissolved in DMSO at 5 mmol/L and diluted with medium to obtain the desired concentration. DMSO concentration in the medium was less than 0.1%. Cells grown in the logarithmic phase were seeded into 96-well plates (4000-6000 cells/well). Twenty-four hours later, quadruplicate wells were untreated or treated with different concentrations of drugs. After incubation for 72 h, 50 μL of MTT solution (10 mg/mL in PBS) was added. Procedure A for the HeLa and SMMC-7721 cell lines: after 4 h of incubation, the medium was removed and replaced with 100 μM DMSO. The plates were shaken for ten minutes and the optical density was measured at a wavelength of 490 nm using a microplate reader (Powerwave XS, Biotek, USA). Procedure B for the K562 cell line: after 4 h of incubation, 100 μM of extraction solution (10% SDS - 5% isobutyl alcohol - 0.01 M HCl) was added. After incubation for 12 h, the optical density was measured at a wavelength of 490 nm using the same microplate reader. Percentages of cell proliferation inhibition versus drug concentrations were plotted. The values shown in table 1 are the means and standard deviations of at least three independent experiments.

4.2.3. Tubulin polymerization assay

Tubulin polymerization assay was conducted using a fluorescence-based tubulin polymerization assay kit (BK011P, Cytoskeleton, USA) according to the manufacturer. Compounds **8c**, **13c** and **13d** were evaluated for their effect on tubulin polymerization. Paclitaxel and CA-4 were used as references, 0.1% DMSO as vehicle control. Compounds at different concentrations were added to the 96-well plate in duplicate. Ater incubation at 37 ^{o}C for 1 min, the icy tubulin reaction mixture (2 mg/mL tubulin in 80 mM PIPES pH 6.9, 2.0 mM $MgCl_2$, 0.5 mM EGTA, 1.0 mM GTP and 15% glycerol) was added. The samples were mixed and tubulin assembly was monitored

(excitation: 360 nm, emission: 450 nm) at 1 min intervals for 1 h at 37 ^{o}C using microplate reader (CLARIOstar, BMG Labtech Inc., Germany). The IC_{50} values were calculated after 40 min.

4.2.4. Immunofluorescence microscopy

HeLa cells were seeded in a 96-well plate at 4000 cells per well and incubated for 24 h. Then the cells were treated with vehicle, **13d** (0.1 μM, 0.15 μM, 0.2 μM) or CA-4 (0.05 μM) for 24 h. The cells were fixed in 4% paraformaldehyde for 10 min at 4 ^{o}C and permeabilized with 0.1% Triton X-100 in PBS for 5 min at 4 ^{o}C. After washed with PBS, cells were blocked with 1% bovine serum albumin (BSA) in PBS for 1h, and incubated with the primary antibody (Catalog No. BM1452, Boster Co. Ltd., China, 1: 100 dilution in 2% BSA-PBS). After incubation for 12 h at 4 ^{o}C, the cells were washed with PBS to remove unbound primary antibody, and incubated with antimouse secondary antibody conjugated with FITC for 30 min at 37 ^{o}C (Catalog No. BA1101, Boster Co. Ltd., China, 1: 100 dilution in 1% BSA-PBS). The cells were washed with PBS to remove unbound secondary antibody, the nuclei were stained with Hoechst 33342 and immunofluorescence was detected using a fluorescence microscope (Leica TCS SP8, Germany).

4.2.5. Cell cycle analyses

HeLa cells were seeded in a 6-well plate at 1×10^5 cells per well and incubated for 24 h. Then the cells were treated with vehicle (0.1% DMSO) or different concentrations of **13d** (0.1 μM, 0.15 μM, 0.2 μM, 0.25 μM) for 24 h. Cells were harvested and fixed with ice-cold 70% ethanol at 4 ^{o}C for 12 h. Ethanol was removed and the cells were washed with cold PBS. Then cells were incubated in 0.5 mL of PBS containing 1 mg/mL Rnase for 30 min at 37 ^{o}C. Then the cells were stained with 50 μg/mL propidium iodide at 4 ^{o}C in the dark for 30 min. The DNA contents of 20000 events were measured by flow cytometer (BD FACSVerse, USA).

4.2.6. Annexin-V assay

Annexin-V assay was conducted using a FITC Annexin-V apoptosis detection kit I (Catalog No. 556547, BD Pharmingen^{TM}, USA). HeLa cells were seeded in a 6-well plate (1×10^5 cells/well). After incubation for 24 h, the cells were treated with vehicle

(0.1% DMSO) or various concentrations of **13d** (0.1 μM, 0.15 μM, 0.2 μM) for 24 h. The cells were harvested and washed with PBS, then the cells were stained with 5 μL of annexin V-FITC and 5 μL PI in binding buffer (10 mM HEPES, 140 mM NaCl and 2.5 mM $CaCl_2$ at pH 7.4) for 15 min at room temperture in the dark. The samples were analyzed using the flow cytometer as mentioned above.

4.2.7. Colchicine competitive binding assay

Tubulin (4 μM, HTS03-A, Cytoskeleton, USA) in buffer containing 80 mM PIPES (pH 6.9), 2 mM $MgCl_2$ and 0.5 mM EGTA was incubated with different concentrations (0.1 μM, 1 μM, 5 μM, 10 μM) of **13d** or paclitaxel at 37 ^{o}C for 1 h in a nontransparent black 96-well plate, with DMSO as control. Then, colchicine (10 μM) was added to the mixture, which was incubated at 37 ^{o}C for an additional 1 h. The fluorescence intensity of the tubulin-colchicine complex (excitation: 340 nm, emission: 435 nm) was measured using a microplate reader (CLARIOstar, BMG Labtech Inc., Germany). Each experiment was performed independently with at least three replicates and expressed as the mean ± SD.

4.3. Molecular modelling

The docking study was carried out using Sybyl-X 2.1. The crystal structure of tubulin complexed with DAMA-colchicine was retrieved from PDB (1SA0). The 3D structure of **13d** was built using Sybyl-X 2.1 and minimized using tripos force field and Gasteiger-Huckel charges. Powell's method was employed with gradient convergence criteria of 0.005 kcal/mol. The DAMA-colchicine structure was extracted and the tubulin structure was prepared and minimized with Amber7 F99 force field. The binding site was constructed by the ligand protomol of surflex dock. Then **13d** was docked into the DAMA-colchicine binding site. The 20 final docked conformations of **13d** were ranked according to the total score. The docking mode was chosen on the basis of total score.

Acknowledgements

The authors are grateful for the financial support from the National Natural Science Foundation of China (No. 21272056, No. U1404819) and Program for

Science Technology Innovation Talents in Universities of Henan Province (16HASTIT029). In additon, this work was also supported by Key Scientific and Technological Projects of Henan Province (Grant No. 132300410228) and Key Scientific Research Program of the Higher Education Institutions of Henan Province (Grant No. 15A350005, Grant No. 2011B310003).

Supplementary material

The ^{1}H and ^{13}C spectra of target compounds.

References

[1] K. N. Bhalla, Microtubule-targeted anticancer agents and apoptosis, Oncogene 22 (2003) 9075-9086.

[2] M. A. Jordan, L. Wilson, Microtubules as a target for anticancer drugs, Nat. Rev. Cancer 4 (2004) 253-265.

[3] C. Dumontet, M. A. Jordan, Microtubule-binding agents: a dynamic field of cancer therapeutics, Nat. Rev. Drug Discov. 9 (2010) 790-803.

[4] C. M. Lin, H. H. Ho, G. R. Pettit, E. Hamel, Antimitotic natural products combretastatin A-4 and combretastatin A-2: Studies on the mechanism of their Inhibition of the binding of colchicine to tubulin, Biochemistry 28 (1989) 6984-6991.

[5] A. T. McGown, B. W. Fox, Differential cytotoxicity of combretastatins A1 and A4 in two daunorubicin-resistant P388 cell lines, Cancer Chemother. Pharmacol. 26 (1990) 79-81.

[6] K. Ohsumi, R. Nakagawa, Y. Fukuda, T. Hatanaka, Y. Morinaga, Y. Nihei, K. Ohishi, Y. Suga, Y. Akiyama, T. Tsuji, Novel combretastatin analogues effective against murine solid tumors: Design and structure-activity relationships, J. Med. Chem. 41 (1998) 3022-3032.

[7] P. E. Thorpe, Vascular targeting agents as cancer therapeutics, Clin. Cancer Res. 10 (2004) 415-427.

[8] S. Aprile, E. Del Grosso, G. C. Tron, G. Grosa, In vitro metabolism study of combretastatin A-4 in rat and human liver microsomes, Drug Metab. Dispos. 35 (2007)

2252-2261.

[9] E. Porcù, R. Bortolozzi, G. Basso, G. Viola, Recent advances in vascular disrupting agents in cancer therapy, Future Med. Chem. 6 (2014) 1485-1498.

[10] G. Bacher, B. Nickel, P. Emig, U. Vanhoefer, S. Seeber, A. Shandra, T. Klenner, T. Beckers, D-24851, a novel synthetic microtubule inhibitor, exerts curative antitumoral activity in vivo, shows efficacy toward multidrug-resistant tumor cells, and lacks neurotoxicity, Cancer Res. 61 (2001) 392-399.

[11] P. Diana, A. Martorana, P. Barraja, A. Montalbano, G. Dattolo, G. Cirrincione, F. Dall'Acqua, A. Salvador, D. Vedaldi, G. Basso, G. Viola, Isoindolo[2,1-*a*]quinoxaline derivatives, novel potent antitumor agents with dual inhibition of tubulin polymerization and topoisomerase□, J. Med. Chem. 51 (2008) 2387-2399.

[12] A. Putey, F. Popowycz, Q. Do, P. Bernard, S. K. Talapatra, F. Kozielski, C. M. Galmarini, B. Joseph, Indolobenzazepin-7-ones and 6-, 8-, and 9-membered ring derivatives as tubulin polymerization inhibitors: synthesis and structure – activity relationship studies, J. Med. Chem. 52 (2009) 5916-5925.

[13] V. Spanò, M. Pennati, B. Parrino, A. Carbone, A. Montalbano, V. Cilibrasi, V. Zuco, A. Lopergolo, D. Cominetti, P. Diana, G. Cirrincione, P. Barraja, N. Zaffaroni, Preclinical activity of new [1,2]oxazolo[5,4-*e*]isoindole derivatives in diffuse malignant peritoneal mesothelioma, J. Med. Chem. 59 (2016) 7223-7238.

[14] H. Mirzaei, S. Emami, Recent advances of cytotoxic chalconoids targeting tubulin polymerization: synthesis and biological activity, Eur. J. Med. Chem. 121 (2016) 610-639.

[15] A. Dowlati, K. Robertson, M. Cooney, W. P. Petros, M. Stratford, J. Jesberger, N. Rafie, B. Overmoyer, V. Makkar, B. Stambler, A. Taylor, J. Waas, J. S. Lewin, K. R. McCrae, S. C. Remick, A phase I pharmacokinetic and translational study of the novel vascular targeting agent combretastatin A-4 phosphate on a single-dose intravenous schedule in patients with advanced cancer, Cancer Res. 62 (2002) 3408-3416.

[16] M. Zweifel, G. C. Jayson, N. S. Reed, R. Osborne, B. Hassan, J. Ledermann, G. Shreeves, L. Poupard, S. P. Lu, J. Balkissoon, D. J. Chaplin, G. J. Rustin, Phase II trial of combretastatin A4 phosphate, carboplatin, and paclitaxel in patients with

platinum-resistant ovarian cancer, Ann. Oncol. 22 (2011) 2036-2041.

[17] Y. Lu, J. Chen, M. Xiao, W. Li, D. D. Miller, An overview of tubulin inhibitors that interact with the colchicine binding site, Pharm. Res. 29 (2012) 2943-2971.

[18] H.-Y. Lee, S.-L. Pan, M.-C. Su, Y.-M. Liu, C.-C. Kuo, Y.-T. Chang, J.-S. Wu, C.-Y. Nien, S. Mehndiratta, C.-Y. Chang, S.-Y. Wu, M.-J. Lai, J.-Y. Chang, J.-P. Liou, Furanylazaindoles: Potent anticancer agents in vitro and in vivo, J. Med. Chem. 56 (2013) 8008-8018.

[19] A. Gangjee, Y. Zhao, S. Raghavan, C. C. Rohena, S. L. Mooberry, E. Hamel, Structure-activity relationship and in vitro and in vivo evaluation of the potent cytotoxic anti-microtubule agent *N*-(4-methoxyphenyl)-*N*,2,6-trimethyl-6,7-dihydro-5*H*-cyclopenta[*d*]pyrimidin-4-aminium chloride and its analogues as antitumor agents, J. Med. Chem. 56 (2013) 6829-6844.

[20] Q. Guan, F. Yang, D. Guo, J. Xu, M. Jiang, C. Liu, K. Bao, Y. Wu, W. Zhang, Synthesis and biological evaluation of novel 3,4-diaryl-1,2,5-selenadiazole analogues of combretastatin A-4, Eur. J. Med. Chem. 87 (2014) 1-9.

[21] R. Kaur, G. Kaur, R. K. Gill, R. Soni, J. Bariwal, Recent developments in tubulin polymerization inhibitors: An overview, Eur. J. Med. Chem. 87 (2014) 89-124.

[22] N. R. Madadi, N. R. Penthala, K. Howk, A. Ketkar, R. L. Eoff, M. J. Borrelli, P. A. Crooks, Synthesis and biological evaluation of novel 4,5-disubstituted 2*H*-1,2,3-triazoles as cis-constrained analogues of combretastatin A-4, Eur. J. Med. Chem. 103 (2015) 123-132.

[23] Z. Wang, H. Qi, Q. Shen, G. Lu, M. Li, K. Bao, Y. Wu, W. Zhang, 4,5-Diaryl-3*H*-1,2-dithiole-3-thiones and related compounds as combretastatin A-4/oltipraz hybrids: Synthesis, molecular modelling and evaluation as antiproliferative agents and inhibitors of tubulin, Eur. J. Med. Chem. 122 (2016) 520-529.

[24] G. R. Pettit, B. Toki, D. L. Herald, P. Verdier-Pinard, M. R. Boyd, E. Hamel, R. K. Pettit, Antineoplastic agents. 379. Synthesis of phenstatin phosphate, J. Med. Chem. 41 (1998) 1688-1695.

[25] D. Rischin, D. C. Bibby, G. Chong, G. Kremmidiotis, A. F. Leske, C. A.

Matthews, S. S. Wong, M. A. Rosen, J. Desai, Clinical, pharmacodynamic, and pharmacokinetic evaluation of BNC105P: a phase I trial of a novel vascular disrupting agent and inhibitor of cancer cell proliferation, Clin. Cancer Res. 17 (2011) 5152-5160.

[26] G. La Regina, R. Bai, W. M. Rensen, E. Di Cesare, A. Coluccia, F. Piscitelli, V. Famiglini, A. Reggio, M. Nalli, S. Pelliccia, E. Da Pozzo, B. Costa, I. Granata, A. Porta, B. Maresca, A. Soriani, M.L. Iannitto, A. Santoni, J. Li, M. Miranda Cona, F. Chen, Y. Ni, A. Brancale, G. Dondio, S. Vultaggio, M. Varasi, C. Mercurio, C. Martini, E. Hamel, P. Lavia, E. Novellino, R. Silvestri, Toward highly potent cancer agents by modulating the C-2 group of the arylthioindole class of tubulin polymerization inhibitors, J. Med. Chem. 56 (2013) 123-149.

[27] J. Zhou, J. Jin, Y. Zhang, Y. Yin, X. Chen, B. Xu, Synthesis and antiproliferative evaluation of novel benzoimidazole-contained oxazole-bridged analogs of combretastatin A-4, Eur. J. Med. Chem. 68 (2013) 222-232.

[28] X. F. Wang, S. B. Wang, E. Ohkoshi, L. T. Wang, E. Hamel, K. Qian, S. L. Morris-Natschke, K. H. Lee, L. Xie, *N*-aryl-6-methoxy-1,2,3,4-tetrahydroquinolines: a novel class of antitumor agents targeting the colchicine site on tubulin, Eur. J. Med. Chem. 67 (2013) 196-207.

[29] Y. T. Duan, Y. L. Sang, J. A. Makawana, S. B. Teraiya, Y. F. Yao, D. J. Tang, X. X. Tao, H. L. Zhu, Discovery and molecular modeling of novel 1-indolyl acetate-5-nitroimidazole targeting tubulin polymerization as antiproliferative agents, Eur. J. Med. Chem. 85 (2014) 341-351.

[30] Y. J. Qin, Y. J. Li, A. Q. Jiang, M. R. Yang, Q. Z. Zhu, H. Dong, H. L. Zhu, Design, synthesis and biological evaluation of novel pyrazoline-containing derivatives as potential tubulin assembling inhibitors, Eur. J. Med. Chem. 94 (2015) 447-457.

[31] M. Gagne-Boulet, S. Fortin, J. Lacroix, C. A. Lefebvre, M. F. Cote, R. C.-Gaudreault, Styryl-*N*-phenyl-*N'*-(2-chloroethyl)ureas and styrylphenylimid-azolidin-2-ones as new potent microtubule-disrupting agents using combretastatin A-4 as model, Eur. J. Med. Chem. 100 (2015) 34-43.

[32] S. F. Wang, Y. Yin, Y. L. Zhang, S. W. Mi, M. Y. Zhao, P. C. Lv, B. Z. Wang, H. L.

Zhu, Synthesis, biological evaluation and 3D-QSAR studies of novel 5-phenyl-1*H*-pyrazol cinnamamide derivatives as novel antitubulin agents, Eur. J. Med. Chem. 93 (2015) 291-299.

[33] D. Renko, O. Provot, E. Rasolofonjatovo, J. Bignon, J. Rodrigo, J. Dubois, J.-D. Brion, A. Hamze, M. Alami, Rapid synthesis of 4-arylchromenes from ortho-substituted alkynols: A versatile access to restricted isocombretastatin A-4 analogues as antitumor agents, Eur. J. Med. Chem. 90 (2015) 834-844.

[34] P. Suman, T. R. Murthy, K. Rajkumar, D. Srikanth, C. Dayakar, C. Kishor, A. Addlagatta, S. V. Kalivendi, B. C. Raju, Synthesis and structure-activity relationships of pyridinyl-1*H*-1,2,3-triazolyldihydroisoxazoles as potent inhibitors of tubulin polymerization, Eur. J. Med. Chem. 90 (2015) 603-619.

[35] Y. T. Wang, Y. J. Qin, N. Yang, Y. L. Zhang, C. H. Liu, H. L. Zhu, Synthesis, biological evaluation, and molecular docking studies of novel 1-benzene acyl-2-(1-methylindol-3-yl)-benzimidazole derivatives as potential tubulin polymerization inhibitors, Eur. J. Med. Chem. 99 (2015) 125-137.

[36] C. Jimenez, Y. Ellahioui, R. Alvarez, L. Aramburu, A. Riesco, M. Gonzalez, A. Vicente, A. Dahdouh, A. Ibn Mansour, D. Martin, R. G. Sarmiento, M. Medarde, E. Caballero, R. Pelaez, Exploring the size adaptability of the B ring binding zone of the colchicine site of tubulin with para-nitrogen substituted isocombretastatins, Eur. J. Med. Chem. 100 (2015) 210-222.

[37] K. Mahal, B. Biersack, S. Schruefer, M. Resch, R. Ficner, R. Schobert, T. Mueller, Combretastatin A-4 derived 5-(1-methyl-4-phenyl-imidazol-5-yl)indoles with superior cytotoxic and anti-vascular effects on chemoresistant cancer cells and tumors, Eur. J. Med. Chem. 118 (2016) 9-20.

[38] M. S. Gerova, S. R. Stateva, E. M. Radonova, R. B. Kalenderska, R. I. Rusew, R. P. Nikolova, C. D. Chanev, B. L. Shivachev, M. D. Apostolova, O. I. Petrov, Combretastatin A-4 analogues with benzoxazolone scaffold: Synthesis, structure and biological activity, Eur. J. Med. Chem. 120 (2016) 121-133.

[39] M. Driowya, J. Leclercq, V. Verones, A. Barczyk, M. Lecoeur, N. Renault, N. Flouquet, A. Ghinet, P. Berthelot, N. Lebegue, Synthesis of triazoloquinazolinone

based compounds as tubulin polymerization inhibitors and vascular disrupting agents, Eur. J. Med. Chem. 115 (2016) 393-405.

[40] V. Spanò, M. Pennati, B. Parrino, A. Carbone, A. Montalbano, A. Lopergolo, V. Zuco, D. Cominetti, P. Diana, G. Cirrincione, N. Zaffaroni, P. Barraja, [1,2]Oxazolo[5,4-*e*]isoindoles as promising tubulin polymerization inhibitors, Eur. J. Med. Chem. 124 (2016) 840-851.

[41] J. Yang, S. Yang, S. Zhou, D. Lu, L. Ji, Z. Li, S. Yu, X. Meng, Synthesis, anti-cancer evaluation of benzenesulfonamide derivatives as potent tubulin-targeting agents, Eur. J. Med. Chem. 122 (2016) 488-496.

[42] D. S. Lawrence, J. E. Copper, C. D. Smith, Structure-activity studies of substituted quinoxalinones as multiple-drug-resistance antagonists, J. Med. Chem. 44 (2001) 594-601.

[43] S. Tanimori, T. Nishimura, M. Kirihata, Synthesis of novel quinoxaline derivatives and its cytotoxic activities, Bioorg. Med. Chem. Lett. 19 (2009) 4119-4121.

[44] B. Bhattacharyya, J. Wolff, Promotion of Fluorescence upon Binding of Colchicine to Tubulin, Proc. Nat. Acad. Sci. U.S.A. 71 (1974) 2627-2631.

[45] X.-F. Wang, F. Guan, E. Ohkoshi, W. Guo, L. Wang, D.-Q. Zhu, S.-B. Wang, L.-T. Wang, E. Hamel, D. Yang, L. Li, K. Qian, S. Morris-Natschke, S. Yuan, K.-H. Lee, L. Xie, Optimization of 4-(*N*-cycloamino)phenylquinazolines as a novel class of tubulin-polymerization inhibitors targeting the colchicine site, J. Med. Chem. 57 (2014) 1390-1402.

[46] A. Kamal, B. Shaik, V. Nayak, B. Nagaraju, J. Kapure, M. Malik, T. Shaik, B. Prasad, Synthesis and biological evaluation of 1,2,3-triazole linked aminocombretastatin conjugates as mitochondrial mediated apoptosis inducers, Bioorg. Med. Chem. 22 (2014) 5155-5167.

[47] R. B. G. Ravelli, B. Gigant, P. A. Curmi, I. Jourdain, S. Lachkar, A. Sobel, M. Knossow, Insight into tubulin regulation from a complex with colchicine and a stathmin-like domain, Nature 428 (2004) 198-202.

List of figures and schemes

Figure 1. CA-4 and its analogues targeting at the colchicine site of tubulin.

Figure 2. (A) Effects of 20 μM **8c**, **13c** and **13d** on tubulin polymerization. Paclitaxel (3 μM) and CA-4 (2.5 μM) were used as reference drugs, 0.1% DMSO as control. (B) Inhibition of tubulin polymerization by **13d** with different concentrations (1 μM, 5 μM, 10 μM, 50 μM).

Figure 3. Fluorescence microscopic images of HeLa cells stained with Hoechst 33342 or anti-α-tubulin-FITC antibody after treatment with 0.1% DMSO, **13d** (0.10 μM, 0.15 μM, 0.20 μM) or CA-4 (0.05 μM) for 24 h.

Figure 4. (A) Flow cytometry analysis of HeLa cells treated with 0.1% DMSO, 0.10 μM, 0.15 μM, 0.20 μM or 0.25 μM compound **13d** for 24 h. (B) The statistical graph of cell cycle distribution.

Figure 5. (A) Bi-parametric histograms of HeLa cells treated with 0.1% DMSO, 0.10 μM, 0.15 μM or 0.20 μM compound **13d** for 24 h by flow cytometry after staining (annexin-V and PI). (B) Percentage of cells found in the different regions of the histograms. (C) Images of cell morphology under the microscope.

Figure 6. Fluorescence based colchicine competitive binding assay. Tubulin (4 μM) was co-incubated with indicated concentrations of paclitaxel or **13d** for 1 h, then 10 μM colchicine was added. Fluorescence values were normalized to control (DMSO).

Figure 7. (A) Comparison between pose of cocrystallized DAMA-colchicine (green) with tubulin and docking poses of **13d**. (B) Proposed binding mode of **13d**. Residues within 3.5 Å of **13d** are shown.

Scheme 1. Reagents and conditions: a) $SOCl_2$, MeOH, 0-50 ^oC; b) amines, EDCI, CH_2Cl_2, rt; c) ethyl bromoacetate, Cs_2CO_3, 140 ^oC; d) 10% Pd/C, H_2, MeOH, rt; e) benzyl chlorides, KI, K_2CO_3, CH_3CN, 70 ^oC; f) LiOH, THF, H_2O, 40 ^oC; g) oxalyl chloride, PhMe, 70 ^oC; amines, K_2CO_3, THF, rt; h) $SOCl_2$, 70 ^oC; i) **12a-e**, K_2CO_3, THF, rt.

List of tables

Table 1. The in vitro antiproliferative activities of synthesized target compounds (**8a-8c**, **9**, **10a**, **10b**, **13a-13l**, doxorubicin and CA-4 against three human cancer cell

lines (HeLa, SMMC-7721 and K562)

Table 1. The in vitro antiproliferative activities of synthesized target compounds (**8a-8c**, **9**, **10a**, **10b**, **13a-13l**, doxorubicin and CA-4 against three human cancer cell lines (HeLa, SMMC-7721 and K562)

Compound	Antiproliferative Activity (IC_{50}, μM)		
	HeLa	SMMC-7721	K562
8a	16.4±1.5	12.5±1.3	43.2±2.9
8b	38.1±5.0	33.2±2.5	43.6±0.7
8c	2.76±0.50	2.69±0.45	3.42±0.85
9	32.2±4.7	39.0±3.9	35.9±8.5
10a	37.5±3.1	39.7±2.3	43.0±7.2
10b	41.8±1.9	28.0±5.4	42.6±4.5
13a	15.9±1.8	7.69±0.35	9.80±2.17
13b	8.28±1.43	5.40±0.78	7.72±2.70
13c	1.42±0.25	1.32±0.22	3.00±1.05
13d	0.126±0.015	0.071±0.014	0.164±0.005
13e	39.4±5.1	9.10±1.68	45.3±3.5
13f	> 50	> 50	> 50
13g	> 50	43.1±7.6	> 50
13h	> 50	40.6±1.7	> 50
13i	24.9±2.4	34.4±3.1	42.9±4.0
13j	26.4±7.4	37.9±8.3	> 50
13k	34.9±7.5	34.9±7.9	> 50
13l	> 50	39.2±7.6	> 50
doxorubicin	1.82±0.31	1.59±0.27	0.89±0.17
CA-4	0.013±0.003	0.0038±0.0020	0.013±0.001

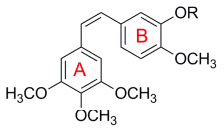

1a （CA-4P）
R = $P(O)O_2Na_2$
1b （CA-4）
R = H

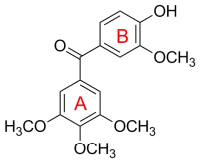

2 (Phenstatin)

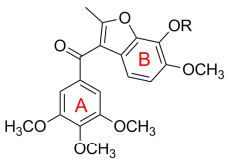

3a （BCN-105）
R = $P(O)O_2Na_2$
3b （BCN-105P）
R = H

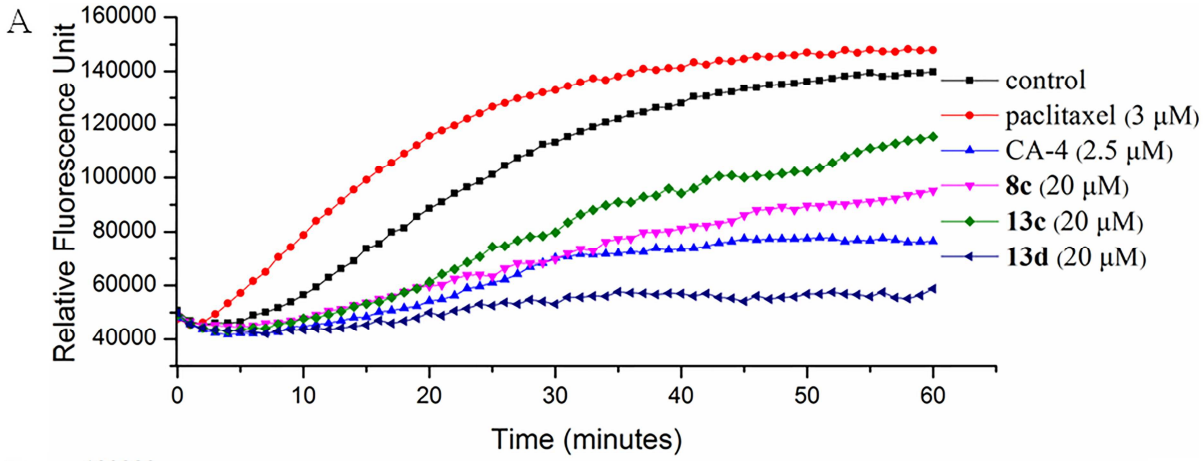
A
Relative Fluorescence Unit
160000
140000
120000
100000
80000
60000
40000
0
10
20
30
40
50
60
Time (minutes)
control
paclitaxel (3 μM)
CA-4 (2.5 μM)
8c (20 μM)
13c (20 μM)
13d (20 μM)

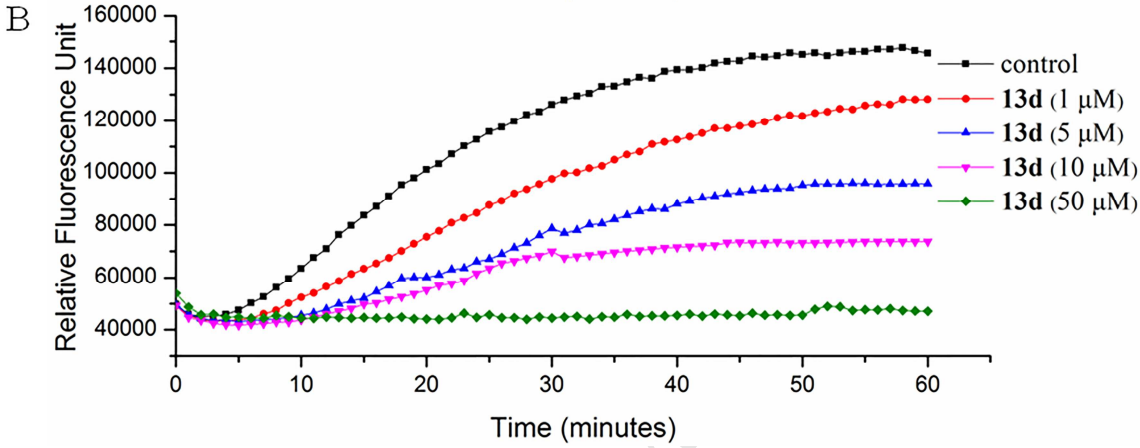
B
Relative Fluorescence Unit
160000
140000
120000
100000
80000
60000
40000
0
10
20
30
40
50
60
Time (minutes)
control
13d (1 μM)
13d (5 μM)
13d (10 μM)
13d (50 μM)

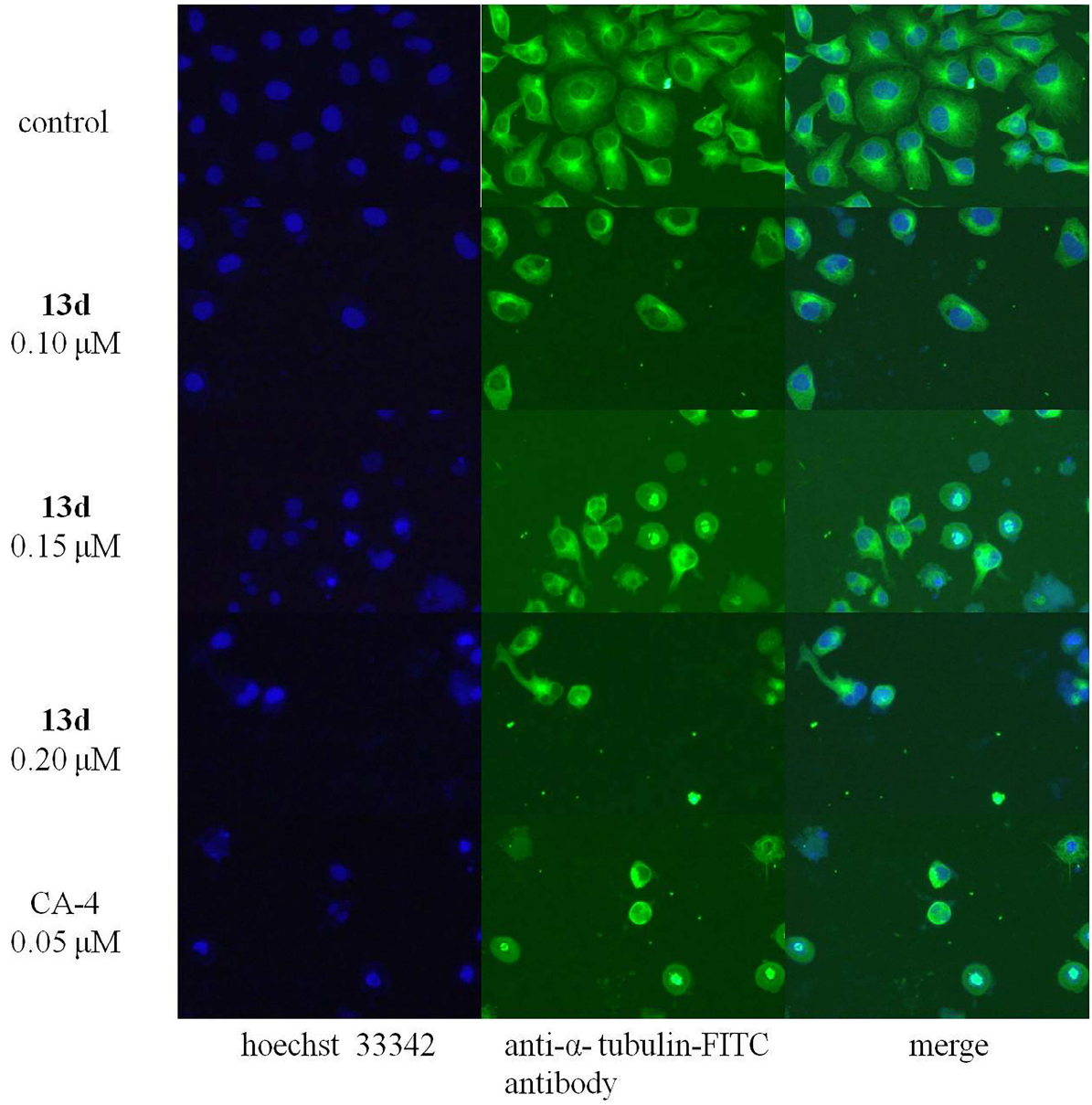
control
13d
0.10 μM
13d
0.15 μM
13d
0.20 μM
CA-4
0.05 μM
hoechst 33342
anti-α- tubulin-FITC antibody
merge

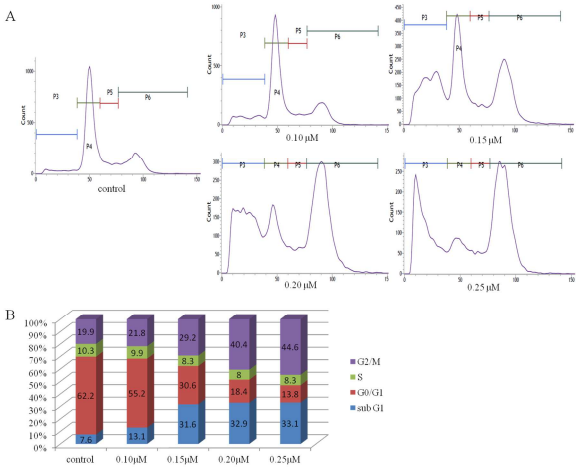

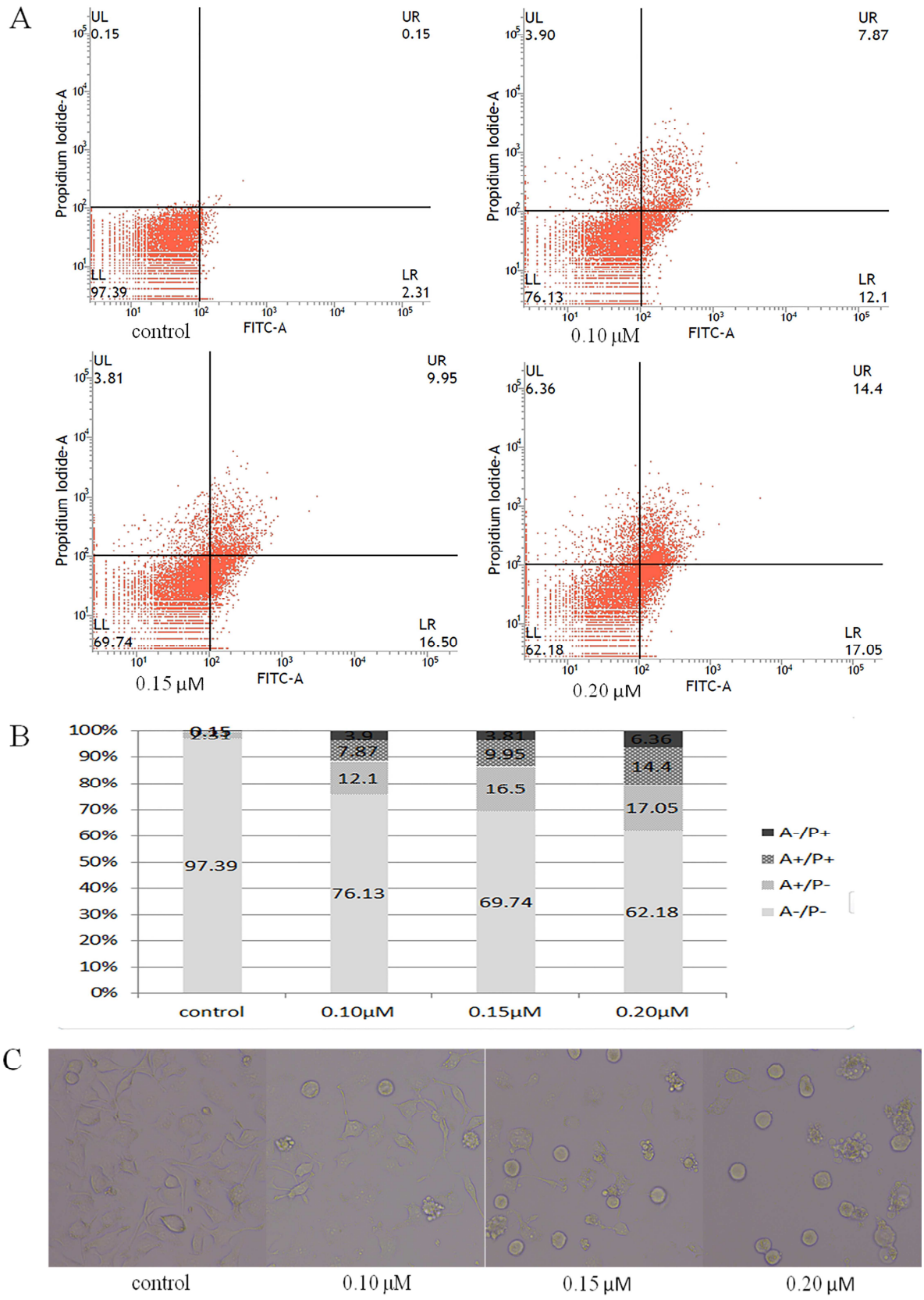
A
UL
0.15
UR
0.15
LL
97.39
LR
2.31
Propidium Iodide-A
FITC-A
control
UL
3.90
UR
7.87
LL
76.13
LR
12.1
0.10 μM
UL
3.81
UR
9.95
LL
69.74
LR
16.50
0.15 μM
UL
6.36
UR
14.4
LL
62.18
LR
17.05
0.20 μM
B
100%
90%
80%
70%
60%
50%
40%
30%
20%
10%
0%
97.39
76.13
69.74
62.18
12.1
16.5
17.05
7.87
9.95
14.4
6.36
control
0.10μM
0.15μM
0.20μM
A-/P+
A+/P+
A+/P-
A-/P-
C
control
0.10 μM
0.15 μM
0.20 μM

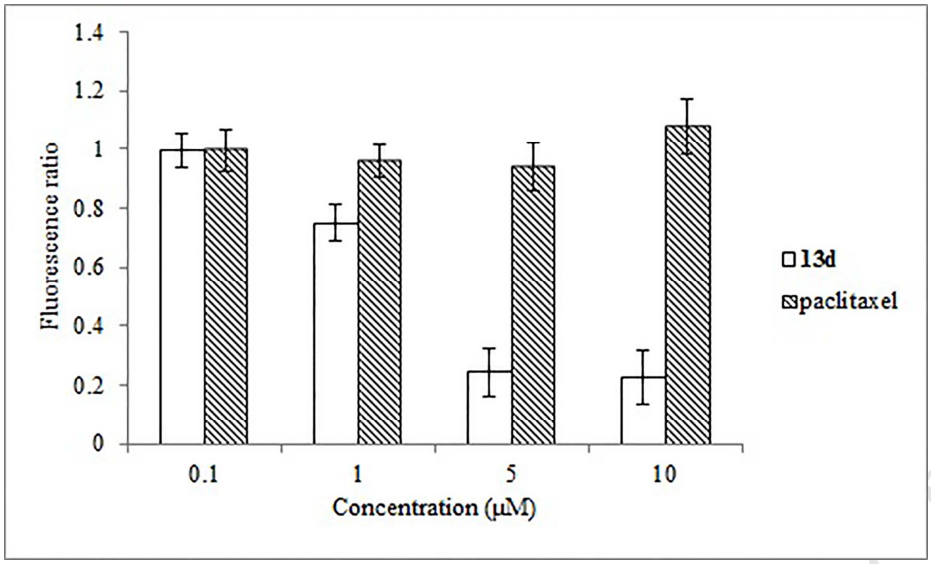

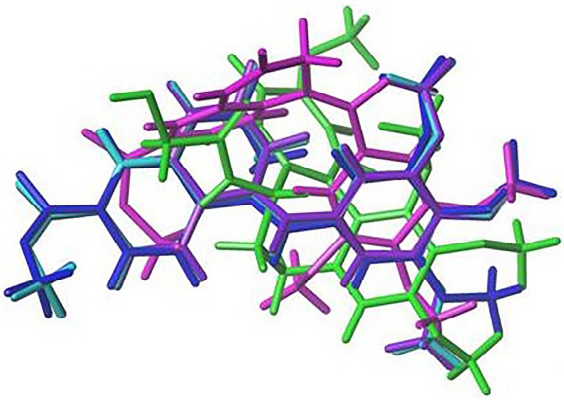

A

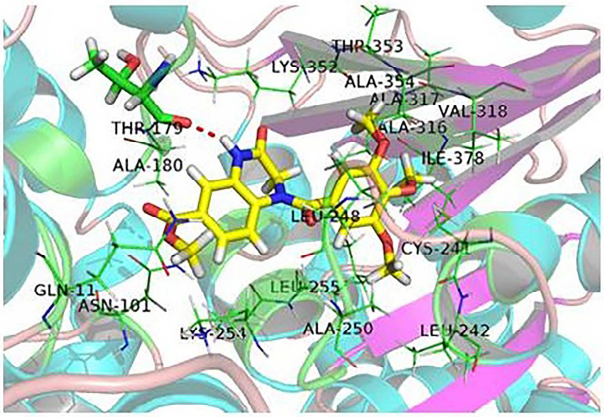

B

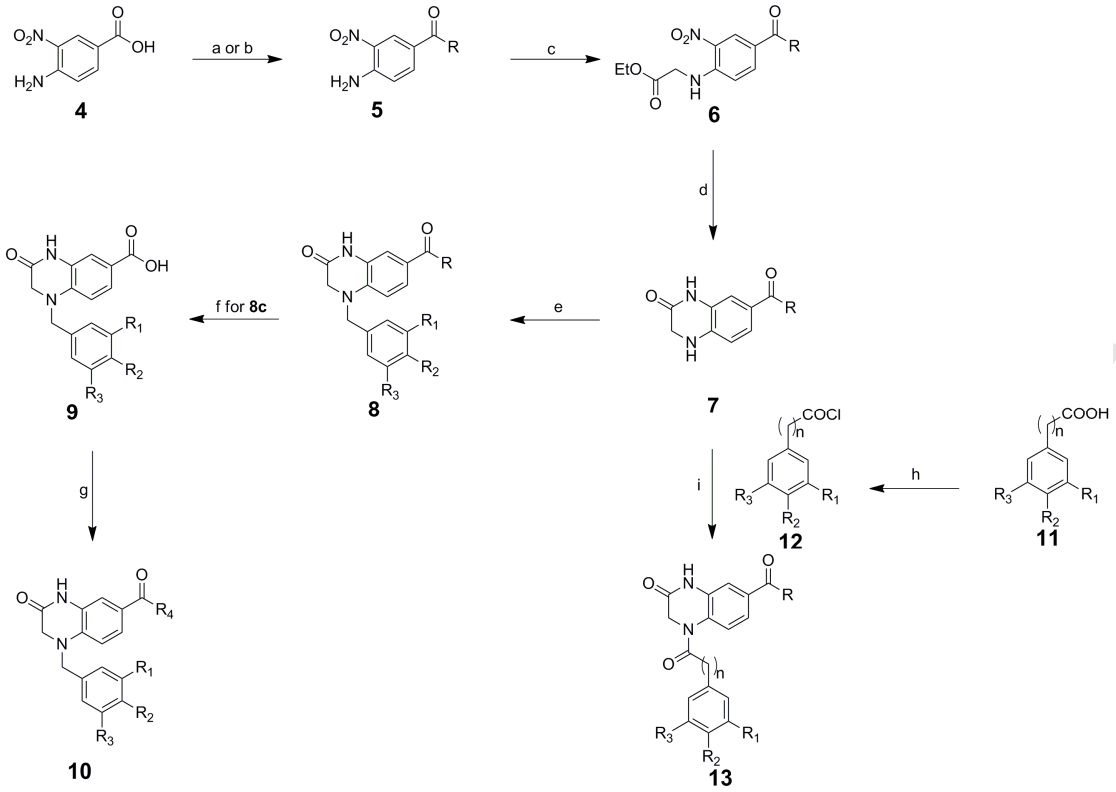

5a/6a/7a: R = $-OCH_3$

5b/6b/7b: R = 

5c/6c/7c: R = 

5d/6d/7d: R = 

5e/6e/7e: R = 

8a: R = R_2 = $-OCH_3$ R_1 = R_3 = -H

8b: R = R_1 = R_2 = $-OCH_3$ R_3 = -H

8c: R = R_1 = R_2 = R_3 = $-OCH_3$

9: R_1 = R_2 = R_3 = $-OCH_3$

10a: R_1 = R_2 = R_3 = $-OCH_3$ R_4 = 

10b: R_1 = R_2 = R_3 = $-OCH_3$ R_4 = 

11a/12a: R_1 = R_3 = -H R_2 = -F n = 0

11b/12b: R_1 = R_3 = -H R_2 = $-OCH_3$ n = 0

11c/12c: R_1 = R_2 = $-OCH_3$ R_3 = -H n = 0

11d/12d: R_1 = R_2 = R_3 = $-OCH_3$ n = 0

11e/12e: R_1 = R_2 = R_3 = $-OCH_3$ n = 1

13a: R = $-OCH_3$ R_1 = R_3 = -H R_2 = -F n = 0

13b: R = $-OCH_3$ R_1 = R_3 = -H R_2 = $-OCH_3$ n = 0

13c: R = $-OCH_3$ R_1 = R_2 = $-OCH_3$ R_3 = -H n = 0

13d: R = $-OCH_3$ R_1 = R_2 = R_3 = $-OCH_3$ n = 0

13e: R = $-OCH_3$ R_1 = R_2 = R_3 = $-OCH_3$ n = 1

13f: R =  R_1 = R_2 = $-OCH_3$ R_3 = -H n = 0

13g: R =  R_1 = R_2 = R_3 = $-OCH_3$ n = 0

13h: R =  R_1 = R_2 = R_3 = $-OCH_3$ n = 0

13i: R =  R_1 = R_2 = $-OCH_3$ R_3 = -H n = 0

13j: R =  R_1 = R_2 = R_3 = $-OCH_3$ n = 0

13k: R =  R_1 = R_2 = $-OCH_3$ R_3 = -H n = 0

13l: R =  R_1 = R_2 = R_3 = $-OCH_3$ n = 0

Highlights

- A series of novel quinoxalinone analogues were synthesized.
- The antiproliferative activities against three cancer cell lines were determined.
- The lead compound **13d** showed IC_{50} values up to nanomolar level.
- **13d** inhibited tubulin polymerization, induced cell cycle arrest and apoptosis.
- The binding site and binding mode of **13d** were probed.